Spectral Self-Coherence Restoral: A New Approach to Blind Adaptive Signal Extraction Using Antenna Arrays

Brian G. Agee
Stephan V. Schell
William A. Gardner

Reprinted from
PROCEEDINGS OF THE IEEE
Vol. 78, No. 4, April 1990

Spectral Self-Coherence Restoral: A New Approach to Blind Adaptive Signal Extraction Using Antenna Arrays

BRIAN G. AGEE, MEMBER, IEEE, STEPHAN V. SCHELL, STUDENT MEMBER, IEEE, AND WILLIAM A. GARDNER, SENIOR MEMBER, IEEE

A new approach to blind adaptive signal extraction using narrowband antenna arrays is presented. This approach has the capability to extract communication signals from co-channel interference environments using only known spectral correlation properties of those signals—in other words, without using knowledge of the content or direction of arrival of the transmitted signal, or the array manifold or background noise covariance of the receiver, to train the antenna array. The class of spectral self-coherence restoral (SCORE) objective functions is introduced, and algorithms for adapting antenna arrays to optimize these objective functions are developed. Using the theory of spectral correlation, it is shown via analysis and simulation that these algorithms maximize the signal-to-interference-and-noise ratio at the output of a narrowband antenna array, when a single communication signal with spectral self-coherence at a known value of frequency separation and an arbitrary number of interferers without spectral self-coherence at that frequency separation are impinging on the array. It is also shown that the SCORE processors can nearly optimally extract communication signals from environments containing multiple signals with spectral self-coherence at the same value of frequency separation.

I. Introduction

The need for blind adaptive signal extraction is growing in a number of signal processing applications. The ability to adapt a receiver processor to remove unknown or time-varying distortion and interference from a signal of interest (SOI), without using knowledge of the transmission channel or waveform to train the processor, can significantly reduce cost and outage time in telephony and microwave communication systems. Blind adaptive processing can also allow signal extraction to be performed in many other applications where it is impractical or impossible to provide such knowledge to the adaptive processor, for example, in mobile radio and in regenerative satellite communication systems, where it can be too costly to provide an adaptive processor with a separate training sequence for each signal received by the transponder or receiver, and in broadcast FM receivers and military reconnaissance and communication systems, where the SOI and interference waveform and channel parameters are typically unknown and time-varying during the reception time.

Antenna arrays provide a particularly useful means for performing this signal extraction in microwave receiver systems, where the most significant signal corruption is caused by co-channel interference. Blind array adaptation algorithms developed to date can be divided into two broad categories: *property restoral* techniques, which adapt arrays to restore a known set of SOI properties to the array output signal, and *spatial-coherence exploitation* techniques, which adapt arrays to exploit known spatial-coherence properties of the signals received by the array. The property restoral technique that has received the most attention in adaptive array applications is the *constant modulus algorithm* [1], [2], which exploits the low modulus variation of most communication signals (for instance, signals with FM, PSK, FSK, and QAM PCM modulation formats). Spatial-coherence exploitation techniques that have been applied to adaptive signal extraction include the *generalized sidelobe canceller* [3] and the *signal subspace techniques*, such as MUSIC [4] and ESPRIT [5], which exploit the discrete spatial distribution of the received signals.

All of the blind adaptation techniques developed to date suffer from shortcomings in practice. The convergence and capture characteristics of the constant modulus algorithm are still not fully understood, a drawback that limits the application of this algorithm in automatic (unsupervised) communication systems where they must operate with a minimum of attention. Although the spatial-coherence exploitation techniques are analytically more tractable, they suffer from other problems associated with measuring the spatial spectrum of the received signal. The generalized sidelobe canceller and MUSIC, for instance, require accurate knowledge of the array manifold to operate, which limits their application in systems where such data are too costly or impossible to measure (for example, if the array

Manuscript received January 16, 1989; revised August 12, 1989. This work was supported in part by a grant from ESL, Inc., with partially matching funds from the California State MICRO Program.

B. G. Agee is with AGI Engineering Consulting, Woodland, CA 95695, U.S.A.

S. V. Schell and W. A. Gardner are with the Dept. of Electrical Engineering and Computer Science, University of California, Davis, CA 95616, U.S.A.

IEEE Log Number 9034609.

0018-9219/90/0400-0753$01.00 © 1990 IEEE

geometry is changing with time), while ESPRIT imposes a structural constraint on the sensor array that can be difficult to satisfy in some practical applications, and that can reduce the degrees of freedom (null-steering capability) of the overall array by as much as 50%. In addition, MUSIC and ESPRIT both require knowledge or estimation of the covariance of the background noise and of the interfering signals that are not to be extracted by the array. This requirement can limit the application of these techniques in environments where the background noise and interference statistics are unknown or varying during the reception time.

All of these techniques suffer from the additional problem that they are nondiscriminatory, and must therefore extract *all* of the unknown signals received by the array and rely on additional downstream processing to separate the SOIs from the interferers. This drawback can be of critical importance in systems where the number of signals impinging on the array is high, especially if only a few of those signals are of interest to the receiver processor.

This paper presents the new class of *spectral self-coherence restoral (SCORE)* algorithms, which have the potential to overcome these limitations. A property held by most communication signals is that they are correlated with frequency-shifted and possibly conjugated versions of themselves for certain discrete values of frequency shift. This property, referred to here as *spectral self-coherence* or *spectral conjugate self-coherence*, is commonly induced by periodic gating, mixing, or multiplexing operations at the transmitter. For instance, spectral self-coherence is induced at multiples of the symbol rate in PCM signals and multiples of the pilot-tone frequency in FDM-FM signals, and spectral conjugate self-coherence is commonly induced at twice the carrier frequency in BPSK and AM signals. The spectral self-coherence of a received signal is degraded if it is corrupted by additive interference that is not spectrally self-coherent at the same value of frequency shift, for instance, if a PCM SOI is corrupted at the receiver by a PCM interferer with a different symbol rate. The SCORE algorithms adapt a receiver array to *restore* this SOI self-coherence, and thereby reduce the power of the interference in the receiver output signal.

Section II introduces the fundamental concepts of spectral self-coherence and conjugate self-coherence, and motivates the development of the SCORE algorithms. Section III introduces the basic SCORE algorithms presented here: the *least-squares SCORE*, *cross-SCORE*, and *auto-SCORE algorithms*. Section IV analyzes the asymptotic (infinite time-average) performance of these algorithms in the *rank-L_α spectral self-coherence* environment where L_α signals with spectral self-coherence or conjugate self-coherence at a target frequency shift α are received by an antenna array. Section V evaluates the performance of the SCORE algorithms in the rank-1 and rank-L_α spectral self-coherence environments via computer simulation.

II. The Spectral Self-Coherence Concept

A scalar waveform $s(t)$ is said to be *spectrally self-coherent at frequency separation* α [6] if the correlation between $s(t)$ and $s(t)$ frequency-shifted by α is nonzero for some lag τ, that is, if

$$\rho_{ss}^{\alpha}(\tau) \triangleq \frac{\langle s(t+\tau/2)[s(t-\tau/2)e^{j2\pi\alpha t}]^*\rangle_\infty}{\sqrt{\langle |s(t+\tau/2)|^2\rangle_\infty \langle |s(t-\tau/2)e^{j2\pi\alpha t}|^2\rangle_\infty}} = R_{ss}^{\alpha}(\tau)/R_{ss}(0) \neq 0 \quad (1)$$

at some value of τ, where $\langle\cdot\rangle_\infty$ denotes infinite time-averaging. Similarly, a signal waveform $s(t)$ is said to be spectrally *conjugate* self-coherent at frequency separation α if the correlation between $s(t)$ and the *conjugate* of $s(t)$ frequency-shifted by α is nonzero for some lag τ, that is, if

$$\rho_{ss^*}^{\alpha}(\tau) \triangleq \frac{\langle s(t+\tau/2)[s^*(t-\tau/2)e^{j2\pi\alpha t}]^*\rangle_\infty}{\sqrt{\langle |s(t+\tau/2)|^2\rangle_\infty \langle |s^*(t-\tau/2)e^{j2\pi\alpha t}|^2\rangle_\infty}} = R_{ss^*}^{\alpha}(\tau)/R_{ss}(0) \neq 0 \quad (2)$$

at some value of τ. The functions $\rho_{ss}^{\alpha}(\tau)$ and $\rho_{ss^*}^{\alpha}(\tau)$ are referred to here as the *spectral self-coherence function* and the *spectral conjugate self-coherence function* of $s(t)$, respectively; the functions $R_{ss}^{\alpha}(\tau)$ and $R_{ss^*}^{\alpha}(\tau)$ are referred to here as the *cyclic autocorrelation function* and the *cyclic conjugate-correlation function* of $s(t)$, respectively, and are defined by

$$R_{ss}^{\alpha}(\tau) \triangleq \langle s(t+\tau/2)s^*(t-\tau/2)e^{-j2\pi\alpha t}\rangle_\infty \quad (3)$$

$$R_{ss^*}^{\alpha}(\tau) \triangleq \langle s(t+\tau/2)s(t-\tau/2)e^{-j2\pi\alpha t}\rangle_\infty. \quad (4)$$

An M-element vector waveform $\mathbf{x}(t)$ is said to be *rank-L_α spectrally self-coherent at frequency separation* α or *rank-L_α spectrally* conjugate *self-coherent at frequency separation* α if the respective cyclic autocorrelation *matrix* $\mathbf{R}_{\mathbf{xx}}^{\alpha}(\tau)$ or cyclic conjugate correlation matrix $\mathbf{R}_{\mathbf{xx}^*}^{\alpha}(\tau)$

$$\mathbf{R}_{\mathbf{xx}}^{\alpha}(\tau) \triangleq \langle \mathbf{x}(t+\tau/2)\mathbf{x}^H(t-\tau/2)e^{-j2\pi\alpha t}\rangle_\infty \quad (5)$$

$$\mathbf{R}_{\mathbf{xx}^*}^{\alpha}(\tau) \triangleq \langle \mathbf{x}(t+\tau/2)\mathbf{x}^T(t-\tau/2)e^{-j2\pi\alpha t}\rangle_\infty \quad (6)$$

has rank L_α ($L_\alpha \leq M$) at frequency-shift α for some lag τ, where T and H denote transpose and conjugate-transpose (Hermitian response) operations, respectively[1].

The spectral self-coherence and conjugate self-coherence properties for a DSB-AM waveform are illustrated in Fig. 1 and Fig. 2, respectively.[2] If the *real* (bandpass representation) signal is under investigation (Fig. 1), then this modulation type has *conjugate-symmetric* frequency content both about its carrier ($f = f_0$) and about DC ($f = 0$). The

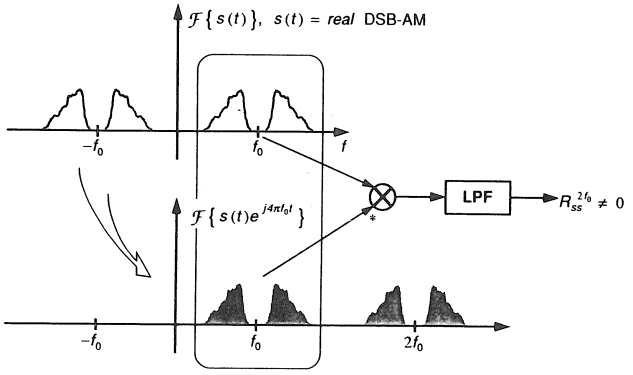

Fig. 1. Spectral self-coherence for a real DSB-AM signal.

[1]The shorthand notation $\mathbf{R}_{(\cdot)}(\tau) \triangleq \mathbf{R}_{(\cdot)}^{\alpha}(\tau)|_{\alpha=0}$, $\mathbf{R}_{(\cdot)}^{\alpha} \triangleq \mathbf{R}_{(\cdot)}^{\alpha}(\tau)|_{\tau=0}$, and $\mathbf{R}_{(\cdot)} \triangleq \mathbf{R}_{(\cdot)}^{\alpha}(\tau)|_{\alpha,\tau=0}$ is used throughout this paper to reduce the level of notation. A similar convention is employed for the spectral self-coherence function $\rho_{(\cdot)}^{\alpha}(\tau)$.

[2]Note that the Fourier transforms shown in these figures are only used as heuristic aids to illustrate the concepts of spectral self-coherence and conjugate self-coherence. Signals that are Fourier transformable cannot exhibit spectral self-coherence, because they cannot have finite average power [7].

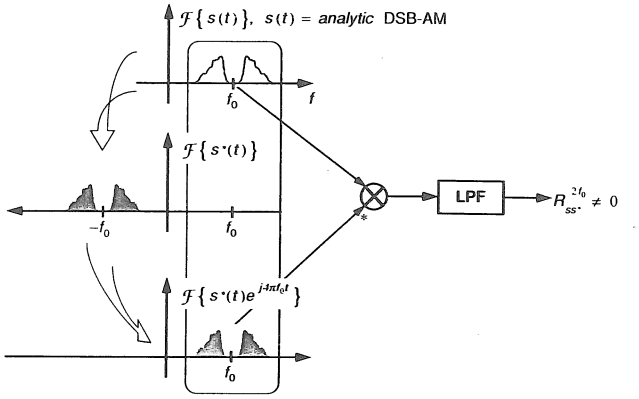

Fig. 2. Spectral conjugate self-coherence for an analytic DSB-AM signal.

combined effect of these symmetries renders the negative-frequency component of the modulated signal equal to the positive-frequency component of the modulated signal, except for a complex phase-shift. The overall signal is therefore correlated with a frequency-shifted version of itself when the frequency shift is exactly equal to twice the signal carrier (Fig. 1), that is, the signal is spectrally self-coherent at $\alpha = 2f_0$.

This correlation can be removed by converting the signal to its *analytic* representation, that is, by removing the negative-frequency signal component using a complex filter. However, the original negative-frequency component can be recreated by *conjugating* the analytic signal, which reflects the signal through the DC axis (Fig. 2). The conjugated signal is then correlated with the original signal after a frequency shift of exactly twice the carrier, that is, the original signal is spectrally *conjugate* self-coherent at $\alpha = 2f_0$.

The spectral self-coherence functions and cyclic correlation functions are developed in detail in the *theory of spectral correlation* [6], [7], where it is shown that complex *wide-sense cyclostationary* and *wide-sense almost-cyclostationary* waveforms exhibit spectral self-coherence or conjugate self-coherence at discrete multiples of the time periodicities of the waveform statistics. Table 1 lists the self-coherence and conjugate self-coherence frequencies for a number of common modulation formats. As this Table shows, this class of waveforms includes most communication signals; for instance, all PCM signals exhibit spectral self-coherence at multiples of their baud-rate, and ASK and BPSK signals are in addition spectrally conjugate self-coherent at twice their carrier frequency. Furthermore, many nominally stationary signals can be spectrally self-coherent if their *baseband* is spectrally self-coherent, for instance, if their baseband is a TDM waveform.

Table 1 Examples of Spectrally Self-Coherent Signals

Complex Modulation Format	Self-Coherence Frequencies	Conj. Self-Coherence Freq. (@ 2 × Carrier)
ASK, BPSK	Baud-rate mult.	Baud-rate mult.
QPSK	Symbol-rate mult.	None
MSK, SQPSK	Baud-rate mult.	± 1/2 baud rate
CPFSK	Symbol-rate mult.	2 × symbol frequencies[a]
FDM-FM	Pilot-tone mult.	None
DSB-AM, VSB-AM	None	2 × carrier
SSB-AM	None	None

[a]frequency deviation = multiple of 1/2 *only*.

The function $|\rho_{ss^{(*)}}^{\alpha}(\tau)|^2$ can be interpreted as a measure of the relative strength of $s(t)$ contained within $s^{(*)}(t-\tau)e^{j2\pi\alpha t}$, where the optional conjugation $(*)$ is only applied if conjugate self-coherence is being measured. Using the Orthogonal Projection Theorem, $s^{(*)}(t-\tau)e^{j2\pi\alpha t}$ can be represented by

$$s^{(*)}(t-\tau)e^{j2\pi\alpha t} = [\rho_{ss^{(*)}}^{\alpha}(\tau)e^{-j\pi\alpha\tau}]^* s(t) + \sqrt{1 - |\rho_{ss^{(*)}}^{\alpha}(\tau)|^2}\,\epsilon_s(t) \tag{7}$$

where $s(t)$ and $\epsilon(t)$ are equal-power orthogonal waveforms ($R_{s\epsilon_s} = 0$). Therefore, $s^{(*)}(t-\tau)e^{j2\pi\alpha t}$ can be thought of as a scaled and corrupted replica of $s(t)$, with a signal-to-corruption ratio of

$$\gamma_{\mathrm{SCR}}^2(\alpha,\tau) \triangleq \frac{|\rho_{ss^{(*)}}^{\alpha}(\tau)|^2}{1 - |\rho_{ss^{(*)}}^{\alpha}(\tau)|^2}. \tag{8}$$

This ratio varies between zero and infinity as $|\rho_{ss^{(*)}}^{\alpha}(\tau)|^2$ varies between zero and unity.

The utility of the self-coherence concept can best be seen in interference environments. Consider the environment where a scalar waveform $x(t)$ is equal to a scaled SOI $s(t)$ plus an independent interference signal $i(t)$, $x(t) = as(t) + i(t)$. If $s(t)$ is spectrally self-coherent at frequency separation α, but $i(t)$ is not spectrally self-coherent at α, then the cyclic autocorrelation of $x(t)$ is given by

$$R_{xx}^{\alpha}(\tau) = |a|^2 R_{ss}^{\alpha}(\tau) + R_{ii}^{\alpha}(\tau) = |a|^2 R_{ss}^{\alpha}(\tau), \tag{9}$$

that is, the infinite time-averaged cyclic autocorrelation of $x(t)$ is unchanged by the addition of *arbitrary* interference, provided that the interference is not spectrally self-coherent at frequency separation α.

A useful interpretation of (9) is that the frequency-shift and optional conjugation operations completely decorrelate the interference component of $x(t)$, but only partially decorrelate the SOI component of $x(t)$. In terms of the decomposition given in (7), $x^{(*)}(t-\tau)e^{j2\pi\alpha t}$ can be expressed in terms of the signal and interference components of $x(t)$ by

$$x^{(*)}(t-\tau)e^{j2\pi\alpha t} = \hat{a}s(t) + \hat{i}(t), \tag{10}$$

where

$$\hat{a} = a\rho_{ss^{(*)}}^{\alpha}(\tau)^* e^{j\pi\alpha\tau} \tag{11}$$

$$\hat{i}(t) = a\sqrt{1 - |\rho_{ss^{(*)}}^{\alpha}(\tau)|^2}\,\epsilon_s(t) + i^{(*)}(t-\tau)e^{j2\pi\alpha t}, \tag{12}$$

and where $\hat{i}(t)$ is uncorrelated with both $s(t)$ and $i(t)$. Equation (10) motivates the development of interference cancellation techniques that use $x^{(*)}(t-\tau)e^{j2\pi\alpha t}$ as the reference signal in a conventional least-squares algorithm.

A different interpretation can be obtained by noting that the spectral self-coherence of $x(t)$ in the above example is reduced when interference that is *not* spectrally self-coherent at shift α is added to the received environment. In this case the self-coherence strength of $x(t)$ is degraded to

$$|\rho_{xx^{(*)}}^{\alpha}(\tau)| = \frac{|\rho_{ss^{(*)}}^{\alpha}(\tau)|}{1 + \mathrm{SINR}^{-1}} \leq |\rho_{ss^{(*)}}^{\alpha}(\tau)| \tag{13}$$

for a signal-to-interference-and-noise ratio of $|a|^2 R_{ss}/R_{ii}$. Equation (13) motivates the development of interference

cancellation techniques that extract SOIs by optimizing some direct or indirect measure of their self-coherence.

III. The SCORE Algorithms

A. Problem Statement

The SCORE algorithms are motivated by extending the example given in Section II to narrowband vector (multisensor) data signals. Consider an environment where an antenna array is excited by a SOI $s(t)$ and by background noise and co-channel interference. If the inverse bandwidth of the receiver is small with respect to the electrical distance between the array elements, then the received signal vector $\mathbf{x}(t)$ can be modelled by

$$\mathbf{x}(t) = \mathbf{a}s(t) + \mathbf{i}(t), \tag{14}$$

where the *SOI aperture vector* $\mathbf{a}$ models the polarization- and direction-of-arrival-dependent antenna gains, cross-sensor phase mismatches, and near-field multipath (scattering) and mutual coupling effects of the array, and where the *interference vector* $\mathbf{i}(t)$ models the remaining signals and background noise received by the array. Assume that $s(t)$ is spectrally self-coherent at α, and that $\mathbf{i}(t)$ is not spectrally self-coherent at α and is temporally uncorrelated with $s(t)$ ($\mathbf{R}_{\mathbf{is}}(\tau) = 0$ for every τ).

Given this model, then $s(t)$ can be extracted from $\mathbf{x}(t)$ using the linear estimator $y(t) = \mathbf{w}^H\mathbf{x}(t)$, where the processor weight vector $\mathbf{w}$ suppresses $\mathbf{i}(t)$ in some manner (for example, by forming an effective antenna pattern with a beam in the direction of $s(t)$ and nulls in the directions of the spatially coherent co-channel interferers). For the environment described in (14), this is optimally accomplished by setting $\mathbf{w}$ equal to a *maximum-SINR* linear combiner

$$\mathbf{w}_{\max} \propto \mathbf{R}_{\mathbf{ii}}^{-1}\mathbf{a} \propto \mathbf{R}_{\mathbf{xx}}^{-1}\mathbf{a}R_{ss}, \tag{15}$$

where $\mathbf{R}_{\mathbf{ii}}$ and $\mathbf{R}_{\mathbf{xx}}$ are the *limit* (infinite time-average) autocorrelation matrices of the interference and received signal vectors. These weights can also be interpreted as the optimal solution to the *least-squares cost function*

$$\mathrm{F}_{\mathrm{LS}}(\mathbf{w}) \triangleq \langle |y(t) - gs(t)|^2 \rangle_\infty, \tag{16}$$

where g is some arbitrary scalar gain constant. Conventional (nonblind) methods for computing $\mathbf{w}_{\max}$ require knowledge of the interference autocorrelation $\mathbf{R}_{\mathbf{ii}}$ or the SOI aperture vector $\mathbf{a}$ to implement (15), or knowledge of the SOI waveform $s(t)$ to minimize (16). The goal in this paper is to adapt $\mathbf{w}$ to approximate (15) without using this knowledge, that is, using only knowledge of the spectral self-coherence properties of the SOI.

B. The Least-Squares SCORE Algorithm

The simplest SCORE algorithm, referred to here as the *least-squares SCORE algorithm*[3], is developed using the interpretation of spectral self-coherence given in (10)–(12). We define a *reference signal* $r(t)$ by

$$r(t) \triangleq \mathbf{c}^H\mathbf{x}^{(*)}(t - \tau)e^{j2\pi\alpha t}, \tag{17}$$

where the vector $\mathbf{c}$ is referred to as the *control vector* and the optional conjugation $(*)$ is applied if and only if conjugate self-coherence is to be restored by the processor. If $\mathbf{x}(t)$ is modeled by (14) and $s(t)$ is the sole received signal component with spectral self-coherence or conjugate self-coherence at frequency separation α, then (10)–(12) can be used to show that $r(t)$ decomposes into a replica of the SOI plus a corruption term that is uncorrelated with both $s(t)$ and $\mathbf{x}(t)$ (and therefore $y(t)$)

$$r(t) = \hat{a}s(t) + \hat{i}(t), \tag{18}$$

where $\hat{a}$ and $\hat{i}(t)$ are given by (11) and (12), respectively, with $a = \mathbf{c}^H\mathbf{a}^{(*)}$ and $i(t) = [\mathbf{c}^{(*)}]^H\mathbf{i}(t)$.

Equation (18) motivates the least-squares SCORE algorithm. We define the *least-squares* SCORE *cost function* by

$$\mathrm{F}_{\mathrm{SC}}(\mathbf{w};\ \mathbf{c}) \triangleq \langle |y(t) - r(t)|^2 \rangle_T, \tag{19}$$

where $y(t) = \mathbf{w}^H\mathbf{x}(t)$ and $r(t)$ is given by (17), and where $\langle \cdot \rangle_T$ denotes time-averaging over the interval $[0, T]$. Substituting (18) into (19) and letting the averaging time grow to infinity yields

$$\begin{aligned}\mathrm{F}_{\mathrm{SC}} &= \langle |y(t) - [\hat{a}s(t) + \hat{i}(t)]|^2 \rangle_T \\ &\to \langle |y(t) - \hat{a}s(t)|^2 \rangle_\infty + \langle |\hat{i}(t)|^2 \rangle_\infty.\end{aligned} \tag{20}$$

Because $\hat{i}(t)$ does not depend on $\mathbf{w}$, it follows that (19) becomes equivalent to the true least-squares cost function (16) and the value of $\mathbf{w}$ that minimizes (19) converges to the maximum-SINR processor as $T \to \infty$.

This result can be proved more directly by solving for the processor vector $\mathbf{w}_{\mathrm{SC}}$ that optimizes (19) for infinite averaging time. Minimizing (19) with respect to $\mathbf{w}$ yields the least-squares SCORE algorithm

$$\mathbf{w}_{\mathrm{SC}} = \hat{\mathbf{R}}_{\mathbf{xx}}^{-1}\hat{\mathbf{R}}_{\mathbf{x}r}, \tag{21}$$

where $\hat{\mathbf{R}}_{\mathbf{xx}}$ and $\hat{\mathbf{R}}_{\mathbf{x}r}$ are the sample autocorelation matrix and cross-correlation vector computed over $[0, T]$. If $\mathbf{i}(t)$ is not spectrally self-coherent at α, then as $T \to \infty$ (21) converges to

$$\mathbf{w}_{\mathrm{SC}} \to \mathbf{R}_{\mathbf{xx}}^{-1}\mathbf{R}_{\mathbf{x}r} \tag{22}$$

$$= \mathbf{R}_{\mathbf{xx}}^{-1}\mathbf{R}_{\mathbf{xx}}^{\alpha}(\tau)\mathbf{c}e^{-j\pi\alpha\tau}. \tag{23}$$

If only $s(t)$ is spectrally self-coherent at α, then as $T \to \infty$, $\mathbf{R}_{\mathbf{xx}}^{\alpha}(\tau)$ reduces to a rank-1 matrix with form

$$\mathbf{R}_{\mathbf{xx}}^{\alpha}(\tau) = \mathbf{a}[\mathbf{a}^{(*)}]^H R_{ss^{(*)}}^{\alpha}(\tau) \tag{24}$$

and (23) reduces to

$$\mathbf{w}_{\mathrm{SC}} \to \mathbf{R}_{\mathbf{xx}}^{-1}(\mathbf{a}[\mathbf{a}^{(*)}]^H\mathbf{c})\,R_{ss^{(*)}}^{\alpha}(\tau)\,e^{-j\pi\alpha\tau} \tag{25}$$

$$= g_{\mathrm{SC}}\mathbf{R}_{\mathbf{xx}}^{-1}\mathbf{a}R_{ss}, \qquad g_{\mathrm{SC}} = [\mathbf{a}^{(*)}]^H\mathbf{c}\rho_{ss^{(*)}}^{\alpha}(\tau)\,e^{-j\pi\alpha\tau}. \tag{26}$$

That is, ω_{SC} reduces to the maximum-SINR (or scaled least-squares) weight vector given by (15), where g_{SC} is the gain constant appearing in (16). Note that $\mathbf{w}$ converges to the maximum-SINR solution for *any* value of $\mathbf{c}$, as long as $\mathbf{c}$ is not orthogonal to $\mathbf{a}^{(*)}$.

The least-squares SCORE processor block diagram is shown in Fig. 3. The reference signal $r(t)$ is generated by linearly combining, delaying, conjugating (if conjugate self-coherence is being exploited), and frequency-shifting the data received by the array. The reference signal is then used as a training signal to adapt the processor vector $\mathbf{w}$ using a least-squares algorithm. The only control parameters used in the processor are the control vector $\mathbf{c}$, the delay τ, the

[3]The least-squares SCORE algorithm was first presented in [8].

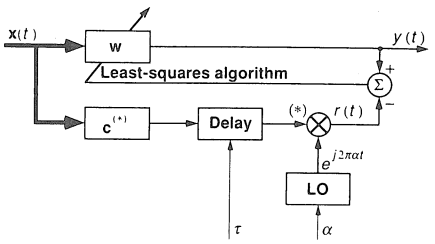

Fig. 3. Least-squares Score processor.

conjugation control, and the frequency-shift α; however, only α and the conjugation control are critical to the operation of the processor. For most communication waveforms much latitude can be allowed in the choice of $\mathbf{c}$ and τ, because in theory these parameters need only be chosen to yield a nonzero value of g_{SC} in (26)[4]. In addition, the frequency-shift parameter α need not be related in any way to the bandwidth or sampling rate of the receiver system; however, care must be taken to avoid aliasing effects if the processor is implemented in digital form and α is large.

From Fig. 3 it is clear that the least-squares SCORE processor can be generalized in several ways. For instance, the delay operation can be replaced by a more general filtering operation, by generating $r(t)$ using

$$r(t) = \mathbf{c}^H \hat{\mathbf{x}}^{(*)}(t) e^{j2\pi\alpha t}, \qquad \hat{\mathbf{x}}(t) = h(t) \otimes \mathbf{x}(t), \tag{27}$$

where $h(t)$ is the *control filter* impulse response and $\otimes$ denotes convolution. The optimum weight vector then converges to

$$\mathbf{w}_{SC} \rightarrow \hat{g}_{SC} \mathbf{R}_{xx}^{-1} \mathbf{a} R_{ss}, \qquad g_{SC} = [\mathbf{a}^{(*)}]^H \mathbf{c} \rho_{s\hat{s}^{(*)}}^{\alpha} \sqrt{\frac{R_{ss}}{R_{\hat{s}\hat{s}}}}, \tag{28}$$

where $\hat{s}(t)$ is the filtered SOI. As Section V shows, a key parameter affecting the convergence rate of the SCORE processor is the strength of the spectral self-coherence $\rho_{s\hat{s}^{(*)}}^{\alpha}$ being restored by the processor; appropriate design of the control filter can improve the performance of the SCORE processor by increasing this strength.

The critical dependence of the SCORE processor on the choice of target α can also be eased somewhat by the particular choice of averaging window used to calculate the finite-time correlation matrices $\hat{\mathbf{R}}_{xx}$ and $\hat{\mathbf{R}}_{xr}$. If a growing rectangular window is used to calculate $\hat{\mathbf{R}}_{xr}$, for instance, then the processor will eventually reject a received SOI if there is *any* error between the self-coherence frequency of the SOI and the target self-coherence frequency of the processor. In many environments, however, the self-coherence frequency of the SOI cannot be known exactly, for instance, if the SOI is subject to Doppler shift (which shifts the conjugate self-coherence frequency of the SOI). The SCORE processor can be made more tolerant to this error if a different choice of averaging window, such as an exponentially decaying window, is used to compute $\hat{\mathbf{R}}_{xr}$.

The greatest improvement in SCORE processor performance can be obtained by adaptively adjusting the control vector as well as the processor vector to some appropriate value. This generalization leads to the *cross-SCORE algorithm*[5], discussed in the next section.

[4]In practice, it is important to choose values of $\mathbf{c}$ and τ that yield a large value of g_{SC}, as this parameter does have a strong effect on the *convergence time* of the SCORE algorithm. This can impose a serious constraint on $\mathbf{c}$ (for example, if the array is subject to strong co-channel interference), but does not impose a strong constraint on τ in most communication applications.

C. The Cross-SCORE Algorithm

An algorithm for adapting $\mathbf{c}$ can be developed by motivating the least-squares SCORE algorithm from a *property-restoral* viewpoint. The same value of $\mathbf{w}_{SC}$ given in (21) results from maximizing the strength of the cross-correlation coefficient between $y(t)$ and $r(t)$

$$\tilde{F}_{SC}(\mathbf{w}; \mathbf{c}) \triangleq |\hat{R}_{yr}|^2 / [\hat{R}_{yy} \hat{R}_{rr}]$$

$$= |\mathbf{w}^H \hat{\mathbf{R}}_{xr}|^2 / [\mathbf{w}^H \hat{\mathbf{R}}_{xx} \mathbf{w} \hat{R}_{rr}] \tag{29}$$

$$= \frac{|\mathbf{w}^H \hat{\mathbf{R}}_{xu} \mathbf{c}|^2}{[\mathbf{w}^H \hat{\mathbf{R}}_{xx} \mathbf{w}][\mathbf{c}^H \hat{\mathbf{R}}_{uu} \mathbf{c}]}, \tag{30}$$

where $\mathbf{u}(t)$ is defined to be the *control signal*,

$$\mathbf{u}(t) \triangleq \hat{\mathbf{x}}^{(*)}(t) e^{j2\pi\alpha t} \Rightarrow r(t) = \mathbf{c}^H \mathbf{u}(t). \tag{31}$$

The cost function $\tilde{F}_{SC}$ is an indirect measurement of the spectral self-coherence in $y(t)$ at frequency separation α; it is lowered if $\mathbf{x}(t)$ contains interference that is not spectrally self-coherent at this frequency separation. In this sense, the least-squares SCORE algorithm can be interpreted as a method for restoring this spectral self-coherence to the processor output signal. The cross-correlation coefficient is also degraded if interference is present in $r(t)$. Consequently, maximizing $\tilde{F}_{SC}$ with respect to $\mathbf{w}$ *and* $\mathbf{c}$ should restore this spectral self-coherence to both $y(t)$ *and* $r(t)$. For this reason, (30) is referred to here as the *cross-SCORE objective function*, and methods for optimizing (30) are referred to here as *cross-SCORE algorithms*.

From the Cauchy-Schwarz Inequality, it is clear that $\mathbf{w}$ is optimized for fixed $\mathbf{c}$ by

$$\mathbf{w}_{opt} \propto \hat{\mathbf{R}}_{xx}^{-1} \hat{\mathbf{R}}_{xr} = \hat{\mathbf{R}}_{xx}^{-1} \hat{\mathbf{R}}_{xu} \mathbf{c}, \tag{32}$$

which is the least-squares SCORE solution (if the delay operation in Fig. 3 is generalized to a filtering equation). Similarly, $\mathbf{c}$ is optimized for fixed $\mathbf{w}$ by

$$\mathbf{c}_{opt} \propto \hat{\mathbf{R}}_{uu}^{-1} \hat{\mathbf{R}}_{ux} \mathbf{w}. \tag{33}$$

Substituting (33) into (30) yields a generalized Rayleigh quotient in $\mathbf{w}$

$$F_{SC}(\mathbf{w}, \mathbf{c}_{opt}) = \frac{\mathbf{w}^H [\hat{\mathbf{R}}_{xu} \hat{\mathbf{R}}_{uu}^{-1} \hat{\mathbf{R}}_{ux}] \mathbf{w}}{\mathbf{w}^H \hat{\mathbf{R}}_{xx} \mathbf{w}}, \tag{34}$$

which is maximized by setting $\mathbf{w}$ equal to the *dominant mode* (eigenvector corresponding to the maximum eigenvalue) of

$$\lambda \hat{\mathbf{R}}_{xx} \mathbf{w} = [\hat{\mathbf{R}}_{xu} \hat{\mathbf{R}}_{uu}^{-1} \hat{\mathbf{R}}_{ux}] \mathbf{w}. \tag{35}$$

Similarly, the control vector is globally optimized by setting $\mathbf{c}$ equal to the dominant mode of

$$\lambda \hat{\mathbf{R}}_{uu} \mathbf{c} = [\hat{\mathbf{R}}_{ux} \hat{\mathbf{R}}_{xx}^{-1} \hat{\mathbf{R}}_{xu}] \mathbf{c}. \tag{36}$$

Equations (35) and (36) are referred to here as *cross-SCORE eigenequations*; both of these eigenequations have the same eigenvalues, with the maximum eigenvalue equal to the maximized objective function value. Equations (35) and

[5]The cross-SCORE algorithm was first presented in [8].

(36) can also be used to obtain an equivalent joint cross-SCORE eigenequation

$$\nu \begin{bmatrix} \hat{\mathbf{R}}_{\mathbf{xx}} & 0 \\ 0 & \hat{\mathbf{R}}_{\mathbf{uu}} \end{bmatrix} \begin{bmatrix} \mathbf{w} \\ \mathbf{c} \end{bmatrix} = \begin{bmatrix} 0 & \hat{\mathbf{R}}_{\mathbf{xu}} \\ \hat{\mathbf{R}}_{\mathbf{ux}} & 0 \end{bmatrix} \begin{bmatrix} \mathbf{w} \\ \mathbf{c} \end{bmatrix}, \tag{37}$$

where $\lambda = \nu^2$ and every solution $(\lambda_k, \mathbf{w}_k, \mathbf{c}_k)$ to (35), (36) has a *pair* of solutions $(\sqrt{\lambda_k}, \mathbf{w}_k, \mathbf{c}_k)$ and $(-\sqrt{\lambda_k}, \mathbf{w}_k, -\mathbf{c}_k)$ to (37).

It is easily shown that the dominant modes of (35) and (36) both converge to the maximum-SINR solution given in (15) if $s(t)$ is the only received signal with spectral self-coherence or conjugate self-coherence at α. In this environment, the Hermitian matrix on the right-hand side of (35) reduces to a rank-1 matrix as $T \to \infty$,

$$\hat{\mathbf{R}}_{\mathbf{xu}} \hat{\mathbf{R}}_{\mathbf{uu}}^{-1} \hat{\mathbf{R}}_{\mathbf{ux}} \to \eta \mathbf{a}\mathbf{a}^H, \qquad \eta = (\mathbf{a}^H \hat{\mathbf{R}}_{\hat{\mathbf{x}}\hat{\mathbf{x}}}^{-1} \mathbf{a}) |R_{ss^{(*)}}^{\alpha}|^2. \tag{38}$$

For an M-element antenna array, the eigenvectors of (35) therefore converge to $M - 1$ *signal-rejection* solutions where $\mathbf{w}$ is orthogonal to $\mathbf{a}$ and λ is equal to zero, and one *signal-selection* solution where $\mathbf{w}$ is equal to $\mathbf{w}_{\max}$ and λ is approximately equal to $|\rho_{ss^{(*)}}^{\alpha}|^2$,

$$\lambda_{\max} \to (\mathbf{a}^H \mathbf{R}_{\mathbf{xx}}^{-1} \mathbf{a})(\mathbf{a}^H \mathbf{R}_{\hat{\mathbf{x}}\hat{\mathbf{x}}}^{-1} \mathbf{a}) |R_{ss^{(*)}}^{\alpha}|^2 \tag{39}$$

$$= \frac{|\rho_{ss^{(*)}}^{\alpha}|^2}{(1 + \gamma_x^{-2})(1 + \gamma_{\hat{x}}^{-2})} \approx |\rho_{ss^{(*)}}^{\alpha}|^2, \qquad \gamma_x^{-2}, \gamma_{\hat{x}}^{-2} \gg 1, \tag{40}$$

where $\gamma_x^2 = \gamma_{\max}^2$ is the maximum-attainable SINR of $s(t)$ for the input data $\mathbf{x}(t)$ and $\gamma_{\hat{x}}^2$ is the maximum-attainable SINR of the filtered SOI $\hat{s}(t)$ for the filtered input data $\hat{\mathbf{x}}(t)$. Similarly, $\hat{\mathbf{R}}_{\mathbf{ux}} \hat{\mathbf{R}}_{\mathbf{xx}}^{-1} \hat{\mathbf{R}}_{\mathbf{xu}}$ reduces to a rank-1 matrix in this environment as $T \to \infty$, and the eigenvectors of (36) converge to $M - 1$ signal-rejection solutions where $\mathbf{c}^H \mathbf{a}^{(*)} = 0$ and one signal-selection solution where $\mathbf{c} \propto \mathbf{R}_{\mathbf{uu}}^{-1} \mathbf{a}^{(*)} R_{\hat{s}\hat{s}}$.

A block diagram of the cross-SCORE processor is shown in Fig. 4. Structurally, the processor is identical to the least-

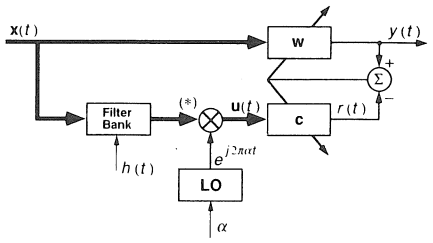

Fig. 4. Cross-Score processor.

squares SCORE processor, except that the control combining is moved to the end of the control path (to allow measurement of $\hat{\mathbf{R}}_{\mathbf{uu}}$ and $\hat{\mathbf{R}}_{\mathbf{xu}}$) and the delay operation is changed to a more general filtering operation. However, in the cross-SCORE processor, both the processor and the control weights are adapted to find the maximum-eigenvalue solution of (37). If only one signal with spectral self-coherence at the target α is incident (or expected) at the array, then the cross-SCORE processor can be very simply implemented using the power method [9]

$$\mathbf{c} \leftarrow g_c \hat{\mathbf{R}}_{\mathbf{uu}}^{-1} \hat{\mathbf{R}}_{\mathbf{ux}} \mathbf{w} \tag{41}$$

$$\mathbf{w} \leftarrow g_w \hat{\mathbf{R}}_{\mathbf{xx}}^{-1} \hat{\mathbf{R}}_{\mathbf{xu}} \mathbf{c}, \tag{42}$$

where g_w and g_c are used to normalize the power of $y(t)$ and $r(t)$ at each step in the algorithm. Equations (41) and (42) converge very rapidly to the dominant mode of (36) in the rank-1 spectral self-coherence environment, because of the wide spread between the maximum and lesser eigenvalues of (37) that prevails in this case.

D. The Auto-SCORE Algorithms

Although the cross-SCORE algorithm can be interpreted as a property-restoral algorithm, it is essentially an extension of the least-squares SCORE algorithm, and as such is motivated more naturally from the interference-decorrelation viewpoint discussed in Section II. A more natural framework for developing a true property-restoral algorithm based on spectral self-coherence is to consider the problem of maximizing the spectral or conjugate self-coherence strength at the output of a *single* linear combiner

$$\hat{F}_{\mathrm{SC}}(\mathbf{w}) \triangleq |\hat{\rho}_{yy^{(*)}}^{\alpha}(\tau)| = \frac{|\mathbf{w}^H \hat{\mathbf{R}}_{\mathbf{xx}}^{\alpha^{(*)}}(\tau) \mathbf{w}^{(*)}|}{\mathbf{w}^H \hat{\mathbf{R}}_{\mathbf{xx}} \mathbf{w}^{(*)}}. \tag{43}$$

Algorithms for optimizing $|\hat{\rho}_{yy}^{\alpha}(\tau)|$ are referred to here as *auto-SCORE algorithms*. Algorithms for optimizing $|\hat{\rho}_{yy^*}^{\alpha}(\tau)|$ are referred to as *conjugate* auto-SCORE algorithms.

A detailed development and discussion of the auto-SCORE and conjugate auto-SCORE algorithms is given in [10] (where they are referred to as the *direct SCORE algorithms*); however, some specific results for these algorithms bear mentioning here. Both classes of algorithms asymptotically (as the averaging time grows to infinity) converge to the maximum-SINR solution in the rank-1 spectral self-coherence environment. In addition, the general (rank-L_α, finite time-average) maximal solution to the conjugate auto-SCORE objective function is nearly always identical to the maximal solution to the analogous conjugate cross-SCORE objective function. In particular, $|\hat{\rho}_{yy^*}^{\alpha}(\tau)|$ is maximized if $\mathbf{w}$ is equal to the dominant mode of

$$\lambda \hat{\mathbf{R}}_{\mathbf{xx}} \mathbf{w} = \tilde{\mathbf{R}}_{\mathbf{xu}} \hat{\mathbf{R}}_{\mathbf{uu}}^{-1} \tilde{\mathbf{R}}_{\mathbf{ux}} \mathbf{w}, \qquad \mathbf{u}(t) = \mathbf{x}^*(t - \tau) e^{j2\pi\alpha t}, \tag{44}$$

where $\tilde{\mathbf{R}}_{\mathbf{xu}}$ is the *symmetrized* cross-correlation between $\mathbf{x}(t)$ and $\mathbf{u}(t)$,

$$\tilde{\mathbf{R}}_{\mathbf{xu}} \triangleq \tfrac{1}{2} [\hat{\mathbf{R}}_{\mathbf{xu}} + \hat{\mathbf{R}}_{\mathbf{ux}}^T]. \tag{45}$$

Equation (44) is identical to the cross-SCORE eigenequation (35) if $\hat{\mathbf{R}}_{\mathbf{xu}}$ is symmetric ($\hat{\mathbf{R}}_{\mathbf{xu}} = \hat{\mathbf{R}}_{\mathbf{xu}}^T$). In fact, in most applications where conjugate self-coherence can be exploited by the processor, $|\rho_{ss^*}^{\alpha}(\tau)|$ is maximized for $\tau = 0$, and the symmetry condition holds. If the symmetry condition does not hold, (45) also shows that a simple modification to eigenequation (37) can transform the cross-SCORE processor to a conjugate auto-SCORE processor.

In contrast, the maximal solutions to the nonconjugated auto-SCORE objective function can differ greatly from the maximal solution to the analogous cross-SCORE objective function under general conditions. In particular, $|\hat{\rho}_{yy}^{\alpha}(\tau)|$ has a local maximum at every dominant mode of

$$\lambda(\varphi) \hat{\mathbf{R}}_{\mathbf{xx}} \mathbf{w} = \tilde{\mathbf{R}}_{\mathbf{xx}}^{\alpha}(\tau, \varphi) \mathbf{w} \tag{46}$$

such that $\lambda_{\max}(\varphi)$ also has a local maximum with respect to φ, where $\tilde{\mathbf{R}}_{\mathbf{xx}}^{\alpha}(\tau, \varphi)$ is the *Hermitianized* cyclic autocorrelation

matrix of $\mathbf{x}(t)$,

$$\tilde{\mathbf{R}}_{\mathbf{xx}}^{\alpha}(\tau, \varphi) \triangleq \tfrac{1}{2}[\hat{\mathbf{R}}_{\mathbf{xx}}^{\alpha}(\tau)e^{-j\varphi} + \hat{\mathbf{R}}_{\mathbf{xx}}^{\alpha}(\tau)^{H}e^{j\varphi}]. \tag{47}$$

A method for adapting $\mathbf{w}$ to perform this optimization is also developed in [10].

A related algorithm has recently been introduced [11] that can be interpreted as a suboptimal solution to the auto-SCORE objective function. This algorithm, referred to here as the *phase-SCORE algorithm*, solves the simpler eigenequation

$$\lambda\hat{\mathbf{R}}_{\mathbf{xx}}\mathbf{w} = \hat{\mathbf{R}}_{\mathbf{xx}}^{\alpha}(\tau)\mathbf{w} \tag{48}$$

for the complex eigenvalue λ with maximum strength $|\lambda|$. As the next sections show, the phase-SCORE algorithm has very attractive analytical, implementation, and performance properties, which give it some inherent advantages over the cross-SCORE algorithm if nonconjugate self-coherence is being restored by the adaptive processor.

The auto-SCORE and conjugate auto-SCORE objective functions can also be generalized by replacing the delay operation with a more flexible filtering operation, yielding

$$\hat{f}_{SC}(\mathbf{w}) \triangleq |\hat{\rho}_{yr}| = \frac{|\mathbf{w}^{H}\hat{\mathbf{R}}_{\mathbf{xu}}\mathbf{w}^{(*)}|}{\sqrt{[\mathbf{w}^{H}\hat{\mathbf{R}}_{\mathbf{xx}}\mathbf{w}][\mathbf{w}^{H}\hat{\mathbf{R}}_{\mathbf{uu}}^{(*)}\mathbf{w}]}} \tag{49}$$

where $\mathbf{u}(t)$ is given by (31), and (with a change from the notation used in the previous sections) $r(t) = [\mathbf{w}^{(*)}]^{H}\mathbf{u}(t)$. However, this filtering approach is less useful here, because $\mathbf{w}$ must achieve a compromise between the optimal extractor of a given SOI from the received environment and the *filtered* SOI from the *filtered* received environment. If the filtering operation affects the SOI and interference differently (for example, if the control filter is selectively nulling the interference), then the resultant processor can diverge significantly from the maximum-SINR processor. The exception to this observation is the phase-SCORE algorithm given by

$$\lambda\hat{\mathbf{R}}_{\mathbf{xx}}\mathbf{w} = \hat{\mathbf{R}}_{\mathbf{xu}}\mathbf{w}, \tag{50}$$

which converges to a maximum-SINR solution in the rank-1 spectral self-coherence environment for any control filter (as long as $\hat{\rho}_{s\hat{s}} \neq 0$).

IV. Analysis of the SCORE Algorithms

A. Infinite-Collect Analysis

The stationary solutions of the SCORE objective functions are easiest to discern under *infinite-collect* conditions where the averaging-time T grows to infinity. Under these conditions, the sample correlation matrices can be replaced with their limit values, and all cross-correlations between statistically uncorrelated signals and signal components can be set equal to zero.

In Section III, it is shown that all of the SCORE algorithms converge to the maximum-SINR solution in the rank-1 spectral self-coherence environment where only one signal with spectral self-coherence at the target α is received by the array. The behavior of the SCORE algorithms in the rank-L_α spectral self-coherence environment remains to be determined, however. This analysis is performed below.

1) Assumed Environment: Consider the environment shown in Fig. 5, where N_α uncorrelated signals $\{s_n(t)\}_{n=1}^{N_\alpha}$ with spectral self-coherence or conjugate self-coherence at

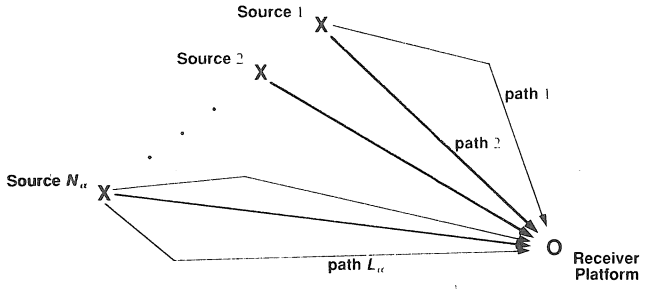

Fig. 5. Rank-L_α collect geometry.

α arrive at an M-element antenna array, together with interference $i(t)$ that is not self-coherent at α. Each signal $s_n(t)$ is assumed to arrive at the receiver along K_n paths, such that $L_\alpha = \Sigma_{n=1}^{N_\alpha} K_n$ signals are received from the N_α separate sources. We denote the kth signal received from the nth source by $s_{kn}(t)$, and assume that this signal arrives at direction θ_{kn} with delay τ_{kn} and scaling coefficient g_{kn}. Then under the narrowband assumption stated in Section III, the received data vector $\mathbf{x}(t)$ is modeled by

$$\mathbf{x}(t) = \sum_{n=1}^{N_\alpha}\left[\sum_{k=1}^{K_l} g_{kn}\mathbf{a}(\theta_{kn})s_{kn}(t - \tau_{kn})\right] + \mathbf{i}(t) \tag{51}$$

$$= \sum_{n=1}^{N_\alpha}\mathbf{A}_n\mathbf{s}_n(t) + \mathbf{i}(t) \tag{52}$$

$$= \mathbf{A}\mathbf{s}(t) + \mathbf{i}(t) \tag{53}$$

where

$$\mathbf{s}_n(t) \triangleq [s_{1n}(t - \tau_{1n}) \cdots s_{K_n n}(t - \tau_{K_n n})]^{T}$$

$$\mathbf{A}_n \triangleq [g_{1n}\mathbf{a}(\theta_{1n}) \cdots g_{K_n n}\mathbf{a}(\theta_{K_n n})]$$

are the *received signal vector* and the *received signal aperture matrix* due to the nth source, and where

$$\mathbf{s}(t) \triangleq [\mathbf{s}_1^{T}(t) \cdots \mathbf{s}_{N_\alpha}^{T}(t)]^{T}$$

$$\mathbf{A} \triangleq [\mathbf{A}_1 \cdots \mathbf{A}_{N_\alpha}]$$

are the received signal vector and received signal aperture matrix due to all of the sources. Similarly, the control signal $\mathbf{u}(t)$ is modeled by

$$\mathbf{u}(t) = \mathbf{A}^{(*)}[\hat{\mathbf{s}}^{(*)}(t)e^{j2\pi\alpha t}] + [\hat{\mathbf{i}}^{(*)}(t)e^{j2\pi\alpha t}] = \tilde{\mathbf{A}}\tilde{\mathbf{s}}(t) + \tilde{\mathbf{i}}(t) \tag{54}$$

where $\tilde{\mathbf{A}} = \tilde{\mathbf{A}}^{(*)}$ and $\tilde{\mathbf{s}}(t)$ and $\tilde{\mathbf{i}}(t)$ are the filtered, optionally conjugated, and frequency-shifted received signal and interference signal vectors.

For the analysis presented here, it is also assumed that $\mathbf{s}(t)$, $\tilde{\mathbf{s}}(t)$, $\mathbf{A}$, and $\tilde{\mathbf{A}}$ have maximal rank, that is, the fully coherent multipath environment is not considered. However, the primary results of this analysis should extend easily to the fully coherent multipath environment, because signal extraction (rather than direction finding) is of interest in this paper.

2) Analysis of the Least-Squares SCORE and Cross-SCORE Algorithms: Analysis of this environment shows that the

least-squares SCORE and cross-SCORE algorithms *screen* the data to optimally suppress the noise and interference $\mathbf{i}(t)$ that is not spectrally self-coherent at the target α, if the total number of received signals that are spectrally self-coherent at α is less than or equal to the number of elements in the array ($L_\alpha \leq M$). Moreover, this analysis also shows that the solutions to the cross-SCORE eigenequation separate the remaining self-coherent signals into N_α blocks, corresponding to selection of each block of correlated signals $\{s_n(t - \tau_{kn})\}_{k=1}^{K_n}$, if $\mathbf{i}(t)$ is low and/or removable by the array and the eigenvalues are distinct between blocks. A corollary of this result is that the cross-SCORE processor can *sort* environments containing multiple uncorrelated signals with spectral self-coherence at the same value of frequency separation, by separating those signals on the basis of their self-coherence strength.

The screening property can be deduced by noting that any processor vector $\mathbf{w}$ can be expressed as the sum of a component that is orthogonal to $\mathbf{A}$ and a component lying in the space spanned by the linear combiners that provide the least-squares estimates of the elements of $\mathbf{s}(t)$ given $\mathbf{x}(t)$. That is, $\mathbf{w}$ can be represented by $\mathbf{w} = \mathbf{w}_s + \mathbf{w}_\perp$, where $\mathbf{w}_\perp$ is in the left null space of $\mathbf{A}$ ($\mathbf{A}^H\mathbf{w}_\perp = \mathbf{0}$) and

$$\mathbf{w}_s \triangleq \mathbf{R}_{xx}^{-1}\mathbf{A}\mathbf{R}_{ss}\mathbf{p}_w \tag{55}$$

$$\Rightarrow \mathbf{p}_w = \mathbf{N}_s^{-1}\mathbf{A}^H\mathbf{w}, \qquad \mathbf{N}_s \triangleq \mathbf{A}^H\mathbf{R}_{xx}^{-1}\mathbf{A}\mathbf{R}_{ss} \tag{56}$$

and where $\mathbf{p}_w = \mathbf{e}_l$ (where $\mathbf{e}_l \triangleq [\delta_{m-l}]_{m=1}^{L_\alpha}$) sets $\mathbf{w}_s$ equal to the least-squares extractor of the lth element of $\mathbf{s}(t)$ from $\mathbf{x}(t)$. Similarly, any control vector $\mathbf{c}$ can be expressed as the sum of a component $\mathbf{c}_\perp$ that is orthogonal to $\tilde{\mathbf{A}}$ ($\tilde{\mathbf{A}}^H\mathbf{c}_\perp = \mathbf{0}$) and a component $\mathbf{c}_s$ lying in the space spanned by the least-squares estimates of the elements of $\tilde{\mathbf{s}}(t)$ given $\mathbf{u}(t)$

$$\mathbf{c}_s = \mathbf{R}_{uu}^{-1}\tilde{\mathbf{A}}\mathbf{R}_{\tilde{s}\tilde{s}}\mathbf{p}_c \tag{57}$$

$$\Rightarrow \mathbf{p}_c = \mathbf{N}_{\tilde{s}}^{-1}\tilde{\mathbf{A}}^H\mathbf{c}, \qquad \mathbf{N}_{\tilde{s}} \triangleq \tilde{\mathbf{A}}^H\mathbf{R}_{uu}^{-1}\tilde{\mathbf{A}}\mathbf{R}_{\tilde{s}\tilde{s}}. \tag{58}$$

Substituting (55) and (57) into the least-squares SCORE equation (22) shows that $y(t) = \mathbf{w}_{SC}^H\mathbf{x}(t)$ lies entirely within the space spanned by the least-squares estimates of $\mathbf{s}(t)$, because

$$\begin{aligned}\mathbf{w}_{SC} &\rightarrow \mathbf{R}_{xx}^{-1}\mathbf{R}_{xu}\mathbf{c}, \qquad \mathbf{R}_{xu} = \hat{\mathbf{A}}\mathbf{R}_{s\tilde{s}}\tilde{\mathbf{A}}^H \\ &= \mathbf{R}_{xx}^{-1}\tilde{\mathbf{A}}\mathbf{R}_{ss}\mathbf{p}_{SC}, \qquad \mathbf{p}_{SC} \triangleq \mathbf{R}_{ss}^{-1}\mathbf{R}_{s\tilde{s}}\tilde{\mathbf{A}}^H\mathbf{c} \\ &= \mathbf{w}_s\end{aligned} \tag{59}$$

for any control vector $\mathbf{c}$. Thus, both the least-squares SCORE algorithm and the cross-SCORE algorithm optimally suppress the background interference $\mathbf{i}(t)$, in the sense that they force $\mathbf{w}_\perp \rightarrow \mathbf{0}$ as $T \rightarrow \infty$.

This property extends to each of the cross-SCORE eigenequation solutions with nonzero eigenvalue. Substituting (55) and (57) into the joint cross-SCORE eigenequation (37) yields the coupled equations

$$\nu[\tilde{\mathbf{A}}\mathbf{R}_{ss}\mathbf{p}_w + \mathbf{R}_{i\tilde{i}}\mathbf{w}_\perp] = \tilde{\mathbf{A}}\mathbf{R}_{s\tilde{s}}\mathbf{N}_{\tilde{s}}\mathbf{p}_c \tag{60}$$

$$\nu[\tilde{\mathbf{A}}\mathbf{R}_{\tilde{s}\tilde{s}}\mathbf{p}_c + \mathbf{R}_{\tilde{i}\tilde{i}}\mathbf{c}_\perp] = \tilde{\mathbf{A}}\mathbf{R}_{\tilde{s}s}\mathbf{N}_s\mathbf{p}_w. \tag{61}$$

Equations (60) and (61) have $2(M - L_\alpha)$ solutions ($M - L_\alpha$ significant solutions) where $\mathbf{p}_w = \mathbf{0} = \mathbf{p}_c$, $(\mathbf{w}, \mathbf{c}) = (\mathbf{w}_\perp, \mathbf{c}_\perp)$, and $\nu = 0$, and $2L_\alpha$ solutions (L_α significant solutions) where $\mathbf{w}_\perp = \mathbf{0} = \mathbf{c}_\perp$ and $(\nu, \mathbf{p}_w, \mathbf{p}_c)$ satisfies the eigenequation

$$\nu\begin{bmatrix}\mathbf{R}_{ss} & \mathbf{0}\\ \mathbf{0} & \mathbf{R}_{\tilde{s}\tilde{s}}\end{bmatrix}\begin{bmatrix}\mathbf{p}_w\\ \mathbf{p}_c\end{bmatrix} = \begin{bmatrix}\mathbf{0} & \mathbf{R}_{s\tilde{s}}\mathbf{N}_{\tilde{s}}\\ \mathbf{R}_{\tilde{s}s}\mathbf{N}_s & \mathbf{0}\end{bmatrix}\begin{bmatrix}\mathbf{p}_w\\ \mathbf{p}_c\end{bmatrix} \tag{62}$$

$$= \begin{bmatrix}\mathbf{0} & \mathbf{R}_{s\tilde{s}}\\ \mathbf{R}_{\tilde{s}s} & \mathbf{0}\end{bmatrix}\begin{bmatrix}\mathbf{N}_s & \mathbf{0}\\ \mathbf{0} & \mathbf{N}_{\tilde{s}}\end{bmatrix}\begin{bmatrix}\mathbf{p}_w\\ \mathbf{p}_c\end{bmatrix}. \tag{63}$$

That is, the joint cross-SCORE eigenequation has $M - L_\alpha$ pairs of *signal-rejection solutions* where the processor and control weight vectors completely reject the signals with self-coherence at α (set $\mathbf{p}_w = \mathbf{0} = \mathbf{p}_c$) and pass the background interference, and L_α pairs of *interference-rejection solutions* where the weight vectors optimally reject the background interference (set $\mathbf{w}_\perp = \mathbf{0} = \mathbf{c}_\perp$) and pass a linear combination of the least-squares estimates of the self-coherent signals. The interference-rejection solutions in effect screen the data and minimize the contribution from any signals that are not spectrally self-coherent or conjugate self-coherent at the target α.

The cross-SCORE sorting property can be deduced from examination of (63) when the background interference is low and/or removable. Using the Matrix Inverse Lemma [9],

$$(\mathbf{C} + \mathbf{A}\mathbf{S}\mathbf{A}^H)^{-1} = \mathbf{C}^{-1} - \mathbf{C}^{-1}\mathbf{A}\mathbf{S}(\mathbf{I} + \mathbf{A}^H\mathbf{C}^{-1}\mathbf{A}\mathbf{S})^{-1}\mathbf{A}^H\mathbf{C}^{-1} \tag{64}$$

$\mathbf{N}_s$ and $\mathbf{N}_{\tilde{s}}$ can be rewritten as

$$\begin{aligned}\tilde{\mathbf{A}}^H\mathbf{R}_{xx}^{-1}\tilde{\mathbf{A}}\mathbf{R}_{ss} &= (\mathbf{I}_{L_\alpha} + \boldsymbol{\Gamma}_s^{-1})^{-1}, \qquad \boldsymbol{\Gamma}_s \triangleq \tilde{\mathbf{A}}^H\mathbf{R}_{ii}^{-1}\tilde{\mathbf{A}}\mathbf{R}_{ss} \\ &= \mathbf{I}_{L_\alpha} - (\mathbf{I}_{L_\alpha} + \boldsymbol{\Gamma}_s)^{-1}\end{aligned} \tag{65}$$

$$\begin{aligned}\tilde{\mathbf{A}}^H\mathbf{R}_{uu}^{-1}\tilde{\mathbf{A}}\mathbf{R}_{\tilde{s}\tilde{s}} &= (\mathbf{I}_{L_\alpha} + \boldsymbol{\Gamma}_{\tilde{s}}^{-1})^{-1}, \qquad \boldsymbol{\Gamma}_{\tilde{s}} \triangleq \tilde{\mathbf{A}}^H\mathbf{R}_{\tilde{i}\tilde{i}}^{-1}\tilde{\mathbf{A}}\mathbf{R}_{\tilde{s}\tilde{s}} \\ &= \mathbf{I}_{L_\alpha} - (\mathbf{I}_{L_\alpha} + \boldsymbol{\Gamma}_{\tilde{s}})^{-1}\end{aligned} \tag{66}$$

where $\boldsymbol{\Gamma}_s$ and $\boldsymbol{\Gamma}_{\tilde{s}}$ can be interpreted as matrix measures of the maximum signal-to-noise-and-interference ratios attainable using an adaptive array on $\mathbf{x}(t)$ and $\mathbf{u}(t)$, respectively. The matrix SINR $\boldsymbol{\Gamma}_s$ is related to the minimum-attainable mean-square error between the lth element of $\mathbf{s}(t)$ and $\mathbf{w}^H\mathbf{x}(t)$ according to the formula [10]

$$\mathrm{MSE}_{\min}(l) = \mathbf{e}_l^H(\mathbf{I}_{L_\alpha} + \boldsymbol{\Gamma}_s)^{-1}\mathbf{e}_l R_{s_l s_l} \tag{67}$$

with an analogous result holding for $\boldsymbol{\Gamma}_{\tilde{s}}$. It is reasonable to assume that $\boldsymbol{\Gamma}_s$ and $\boldsymbol{\Gamma}_{\tilde{s}}$ are usually large ($\|\boldsymbol{\Gamma}_s^{-1}\|, \|\boldsymbol{\Gamma}_{\tilde{s}}^{-1}\| \ll 1$) when the true maximum-attainable SINRs of the self-coherent signals are high, allowing (63) to be approximated by

$$\nu\begin{bmatrix}\mathbf{R}_{ss} & \mathbf{0}\\ \mathbf{0} & \mathbf{R}_{\tilde{s}\tilde{s}}^{(*)}\end{bmatrix}\begin{bmatrix}\mathbf{p}_w\\ \mathbf{p}_c\end{bmatrix} = \begin{bmatrix}\mathbf{0} & \mathbf{R}_{s\tilde{s}}\\ \mathbf{R}_{\tilde{s}s} & \mathbf{0}\end{bmatrix}(\mathbf{I}_{2L_\alpha} - \boldsymbol{\Delta})\begin{bmatrix}\mathbf{p}_w\\ \mathbf{p}_c\end{bmatrix} \tag{68}$$

$$\approx \begin{bmatrix}\mathbf{0} & \mathbf{R}_{s\tilde{s}}\\ \mathbf{R}_{\tilde{s}s} & \mathbf{0}\end{bmatrix}\begin{bmatrix}\mathbf{p}_w\\ \mathbf{p}_c\end{bmatrix} \tag{69}$$

where

$$\boldsymbol{\Delta} = \left(\mathbf{I}_{2L_\alpha} + \begin{bmatrix}\boldsymbol{\Gamma}_s & \mathbf{0}\\ \mathbf{0} & \boldsymbol{\Gamma}_{\tilde{s}}\end{bmatrix}\right)^{-1}$$

$$\rightarrow \mathbf{0} \text{ as } \|\boldsymbol{\Gamma}_s^{-1}\|, \|\boldsymbol{\Gamma}_{\tilde{s}}^{-1}\| \rightarrow 0. \tag{70}$$

Eigenequation (69) can be transformed into separate eigenequations in terms of the individual vectors $\mathbf{p}_w$ and $\mathbf{p}_c$,

$$\lambda \mathbf{R}_{ss} \mathbf{p}_w = [\mathbf{R}_{s\bar{s}} \mathbf{R}_{\bar{s}\bar{s}}^{-1} \mathbf{R}_{s\bar{s}}^H] \mathbf{p}_w \tag{71}$$

$$\lambda \mathbf{R}_{\bar{s}\bar{s}} \mathbf{p}_c = [\mathbf{R}_{s\bar{s}}^H \mathbf{R}_{ss}^{-1} \mathbf{R}_{s\bar{s}}] \mathbf{p}_c, \tag{72}$$

where $\lambda = \nu^2$. Equations (69)–(72) have the same form as the actual cross-SCORE eigenequations, but are expressed directly in terms of the correlation matrices of the underlying received signal vectors $\mathbf{s}(t)$ and $\bar{\mathbf{s}}(t)$.

If multipath is *not* present in the received environment, that is, if the received signals $\{s_l(t - \tau_l)\}_{l=1}^{L_\alpha}$ are uncorrelated ($N_\alpha = L_\alpha$), then the received signal correlation matrices are diagonal, and both (71) and (72) reduce to

$$\lambda \mathbf{p}_{(\cdot)} = \text{diag}\ \{|\rho_{s_l \bar{s}_l}|^2\}\ \mathbf{p}_{(\cdot)} \tag{73}$$

$$= \text{diag}\ \{|\rho^\alpha_{s_l \bar{s}_l}|^2\}\ \mathbf{p}_{(\cdot)}. \tag{74}$$

where $\rho^\alpha_{s_l \bar{s}_l}$ is the cyclic cross-coherence between $s_l(t)$ and $\bar{s}_l^{(*)}(t)$. If the self-coherence strengths $\{|\rho^\alpha_{s_l \bar{s}_l}|^2\}_1^{L_\alpha}$ are *distinct*, then (74) has L_α unambiguous solutions (λ, $\mathbf{p}_w$, $\mathbf{p}_c$) of the form

$$\lambda(l) = |\rho^\alpha_{s_l \bar{s}_l}|^2 \tag{75}$$

$$\mathbf{p}_w(l) = \mathbf{e}_l \tag{76}$$

$$\mathbf{p}_c(l) = \mathbf{e}_l. \tag{77}$$

That is, the cross-SCORE eigenequation has L_α unambiguous solutions, each corresponding to least-squares extraction of each of the received signals $s_l(t - \tau_l)$ from the received environment if those signals have distinct self-coherence strengths and sufficiently high maximum-attainable SINR.

If multipath *is* present in the received environment, such that the self-coherent signals can be grouped into $N_\alpha < L_\alpha$ blocks of correlated signals as shown in Fig. 5, then $\mathbf{R}_{ss}$, $\mathbf{R}_{\bar{s}\bar{s}}$ and $\mathbf{R}_{s\bar{s}}$ are block-diagonal and (71)–(72) reduce to

$$\lambda\ \text{diag}\ \{\mathbf{R}_{s_n s_n}\}\ \mathbf{p}_w = \text{diag}\ \{\mathbf{R}_{s_n \bar{s}_n} \mathbf{R}_{\bar{s}_n \bar{s}_n}^{-1} \mathbf{R}_{s_n \bar{s}_n}^H\}\ \mathbf{p}_w \tag{78}$$

$$\lambda\ \text{diag}\ \{\mathbf{R}_{\bar{s}_n \bar{s}_n}\}\ \mathbf{p}_c = \text{diag}\ \{\mathbf{R}_{s_n \bar{s}_n}^H \mathbf{R}_{s_n s_n}^{-1} \mathbf{R}_{s_n \bar{s}_n}\}\ \mathbf{p}_c. \tag{79}$$

If the eigenvalues of (78) and (79) are distinct, then these eigenequations have N_α blocks of solutions, where the nth block has form

$$\{\lambda(k, n), \mathbf{p}_w(k, n), \mathbf{p}_c(k, n)\}_{k=1}^{K_n}$$

$$= \left\{ \lambda(k, n) \begin{bmatrix} \vdots \\ 0 \\ \hat{\mathbf{p}}_w(k, n) \\ 0 \\ \vdots \end{bmatrix} \begin{bmatrix} \vdots \\ 0 \\ \hat{\mathbf{p}}_c(k, n) \\ 0 \\ \vdots \end{bmatrix} \right\}_{k=1}^{k_n} \tag{80}$$

and where $\{\hat{\mathbf{p}}_w\}$ and $\{\hat{\mathbf{p}}_c\}$ are K_n-dimensional eigenvectors and $\{\lambda(k, n), \hat{\mathbf{p}}_w(k, n), \hat{\mathbf{p}}_c(k, n)\}_{k=1}^{K_n}$ are the solutions to the N_α eigenequations

$$\lambda \mathbf{R}_{s_n \hat{s}_n} \hat{\mathbf{p}}_w = [\mathbf{R}^\alpha_{s_n \hat{s}_n} \mathbf{R}_{\hat{s}_n \hat{s}_n}^{-1} (\mathbf{R}^\alpha_{s_n \hat{s}_n})^H] \hat{\mathbf{p}}_w \tag{81}$$

$$\lambda \mathbf{R}_{\hat{s}_n \hat{s}_n} \hat{\mathbf{p}}_c = [(\mathbf{R}^\alpha_{s_n \hat{s}_n})^H \mathbf{R}_{\hat{s}_n \hat{s}_n}^{-1} \mathbf{R}^\alpha_{s_n \hat{s}_n}] \hat{\mathbf{p}}_c. \tag{82}$$

That is, the cross-SCORE eigenequation divides into N_α *blocks* of solutions, where the nth block of solutions extracts a linear combination of the received signals $\{s_{kn}(t)\}_{k=1}^{K_n}$ associated with the nth signal source, and optimally rejects the background interference and the other uncorrelated SOIs that are self-coherent at α.

Identification of the multipath blocks can be performed by analyzing the structure of the output-signal covariance matrix $\mathbf{R}_{yy} = \mathbf{W}_\alpha^H \mathbf{R}_{xx} \mathbf{W}_\alpha$ where $\mathbf{W}_\alpha$ is the matrix of processor eigenvectors with nonzero eigenvalues at the target α. The output-signal covariance matrix should be block-diagonal with N_α blocks, allowing determination of both the number of sources N_α with spectral self-coherence or conjugate self-coherence at α and the number of received signals per source $\{K_n\}_{n=1}^{N_\alpha}$. Thus, although the cross-SCORE processor is not generally able to correct multipath, it is able to sort the received environment into a set of *multipath blocks* for each transmitted SOI. The sorted multipath blocks can then be passed to a second blind processing stage, such as a constant modulus algorithm [1], to reconstruct the original source.

3) Analysis of the Auto-SCORE Algorithms: The infinite-collect analysis of the auto-SCORE objective function is straightforward and parallels the analysis of the cross-SCORE objective function[6]. In particular, if the general environment given in (53) is assumed, and $\mathbf{u}(t)$ is formed without a conjugation operation, then $\bar{\mathbf{A}} = \mathbf{A}$ and the phase-SCORE eigenequation given in (50) transforms to

$$\lambda[\mathbf{A} \mathbf{R}_{ss} \mathbf{p}_w + \mathbf{R}_{ii} \mathbf{w}_\perp] = \mathbf{A} \mathbf{R}_{s\bar{s}} \mathbf{N}_s \mathbf{p}_w \tag{83}$$

under the representation (55) for $\mathbf{w}$. Equation (83) has $M - L_\alpha$ solutions where $\mathbf{p}_w = \mathbf{0}$, $\mathbf{w} = \mathbf{w}_\perp$ and $\lambda = 0$, and L_α solutions where $\mathbf{w}_\perp = \mathbf{0}$ and (λ, $\mathbf{p}_w$) satisfies

$$\lambda \mathbf{R}_{ss} \mathbf{p}_w = \mathbf{R}_{s\bar{s}} [\mathbf{I}_{L_\alpha} - (\mathbf{I}_{L_\alpha} - \boldsymbol{\Gamma}_s)^{-1}] \mathbf{p}_w \tag{84}$$

$$\rightarrow \mathbf{R}_{s\bar{s}} \mathbf{p}_w, \qquad \|\boldsymbol{\Gamma}_s^{-1}\| \ll 1. \tag{85}$$

The phase-SCORE eigenequation shown in (85) is discussed extensively in [10], [11], where it is used to show that the phase-SCORE eigenvectors share the screening and sorting properties exhibited by the cross-SCORE eigenvectors. However, the phase-SCORE eigenequation also possesses several important advantages over the cross-SCORE eigenequation, due to its having a complex-valued eigenvalue, that are worth noting here. In particular, if $\|\boldsymbol{\Gamma}_s^{-1}\| \ll 1$ and $\{s_l(t)\}_1^{L_\alpha}$ are independent and identically distributed signals (for example, if the signals are part of a communications net) and $L_\alpha \leq M$, then $\mathbf{R}_{s\bar{s}}$ is diagonal and (85) has L_α nonzero solutions associated with selection of each of the self-coherent signals with $\lambda(l) = \rho_{s_l \bar{s}_l}$, as long as those signals have distinct self-coherence strengths *or phases* (for example, caused by different timing phases). This is in contrast to the cross-SCORE eigenequation, which can only separate signals if they have distinct self-coherence strengths. The phase-SCORE eigenequation can also be shown to have N_α blocks of nonzero solutions corresponding to selection of each block of correlated self-coherent signals in the multipath environment discussed above. In [10], it is also shown that many of these results also extend to the auto-SCORE objective function. In particular, the auto-SCORE objective function possesses the same screening and sorting properties exhibited by the phase-SCORE algorithms.

[6]The behavior of the conjugate auto-SCORE objective function is not of concern here, as it is equivalent to a slightly modified (and usually identical) conjugate cross-SCORE eigenequation.

The dependence of the phase-SCORE eigenequation and the auto-SCORE stationary solutions on the phase as well as the strength of the spectral self-coherence of the received signals significantly broadens the applications of these algorithms, as the received signals rarely have identical timing phase even if they have identical structure. This property can also improve the convergence characteristics of the approach, as discussed in the next section.

B. Finite-Collect Analysis

A rigorous analysis of the performance of the SCORE algorithms under *finite-collect conditions* is beyond the scope of this paper. However, some qualitative statements can be made here.

In the rank-1 spectral self-coherence environment, both the least-squares SCORE algorithm and the power-method cross-SCORE algorithm described in Section III can be treated as *noisy least squares algorithms*, where the training (reference) signal $r(t)$ is equal to a desired signal $\hat{a}s(t)$ corrupted by uncorrelated additive noise $\hat{i}(t)$. Until $\hat{i}(t)$ is averaged out by the correlation process, this corruption component can have a strong effect on the adaptation of the processor weights.

This noise component is dominated by the background interference in the least-squares SCORE algorithm if $\mathbf{c}$ is chosen arbitrarily. Thus, the least-squares SCORE algorithm should converge slowly (with respect to a nonblind algorithm that uses $r(t) = s(t)$ to train the processor) if the background interference is strong and is not removed by the control combiner, regardless of the self-coherence strength of the SOI being selected by the processor.

In contrast, the performance of the cross-SCORE processor should be strongly dependent on the strength of the SOI self-coherence. Adaptation of the control vector during the optimization process removes the bulk of the background interference from the control path, leaving only the self-interference component given in (12), which cannot be removed because it has the same direction of arrival as the SOI. As (8) shows, the reciprocal strength $\gamma^2_{\mathrm{SCR}}(\alpha, \tau)$ of the self-corruption component is directly dependent on $|\rho^{\alpha}_{s\hat{s}^{(*)}}|$; if $|\rho^{\alpha}_{s\hat{s}^{(*)}}|$ is close to unity then $\gamma^2_{\mathrm{SCR}}(\alpha, \tau)$ is very large and the algorithm should converge nearly as fast as a nonblind least-squares algorithm. However, if $|\rho^{\alpha}_{s\hat{s}^{(*)}}| \ll 1$, then $\gamma^2_{\mathrm{SCR}}(\alpha, \tau)$ is small and the cross-SCORE algorithm converges much more slowly than the nonblind least-squares algorithm.

The performance of these algorithms can also be affected by the spectral self-coherence properties of the other signals in the environment, even if the other signals are not truly (for infinite collects) spectrally self-coherent at α. In particular, if the environment contains $\tilde{L}_{\alpha}$ signals that are spectrally self-coherent in the *vicinity* of α, then it is appropriate to treat the environment as *rank-$\tilde{L}_{\alpha}$ self-coherent* until the *cycle resolution* (reciprocal of the collect time) [6] of the spectral correlation measurement becomes narrow enough to discriminate against the other signals. A positive consequence of this observation is that the SCORE algorithms should be able to select signals even if they are not spectrally self-coherent at the target α, given a short enough averaging time or a wide enough cycle resolution. A negative consequence of this result is that the other signals may interfere with the signals of interest at the target α and slow the convergence time of the SCORE processor.

This phenomenon affects the cross-SCORE algorithms more strongly than the auto-SCORE and phase-SCORE algorithms, due to the dependence of the cross-SCORE algorithms on the self-coherence strength of the received signals. The measured spectral self-coherence of the received signals is erratic over short averaging times, and the self-coherence strengths of the signals can coincide and cross at random intervals over the early portion of any collect. The cross-SCORE algorithm is not able to separate the received signals when their measured self-coherence strengths coincide, resulting in random intervals of performance loss, or "signal drop-outs" over the beginning and intermediate portions of the collect. However, the *complex value* (strength *and* phase) of the self-coherence measurements of the received signals should rarely coincide. Consequently, the auto-SCORE and phase-SCORE algorithms should not be subject to the drop-out phenomenon.

V. Performance of the SCORE Algorithms

A. Simulator Setup

The basic collect geometry and received environment for the simulations conducted here are shown in Figs. 6 and

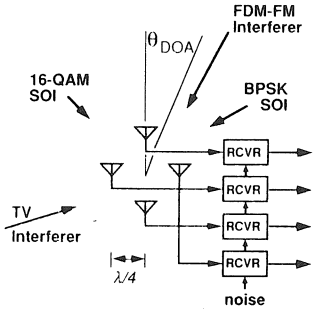

Fig. 6. Receiver front end.

7. A four-element circular array with a 10.24 MHz complex (bandpass) reception bandwidth, isotropic array elements, and a half-wavelength array diameter is excited by white Gaussian noise, two PCM SOIs, and FDM-FM and TV inter-

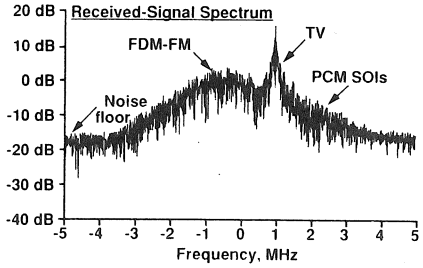

Fig. 7. Received signal environment, isotropic antenna pattern.

ference signals. The Gaussian noise is white in both spatial and frequency domains. The PCM signals are transmitted using Nyquist-shaped modulation pulses with 100% rolloff ($\cos^2((\pi/2)(f/f_s))$ pulse Fourier transforms, where f_s is the symbol rate of the SOI), and with BPSK and 16-QAM symbol constellations. The FDM-FM signal consists of a carrier frequency-modulated by a 120-channel 60-552 kHz noise-loaded baseband with a 200-kHz rms frequency deviation.

The TV signal simulates a horizontal-synchronization pulse-train with a 15.625 kHz (CCIR standard) line rate. The received data vector is converted to complex-baseband representation and sampled at a 10.24 Ms/sec complex sampling rate prior to adaptive processing. The received signal parameters are given in Table 2, where *DOA* denotes *direction of arrival* and *SWNR* denotes *signal-to-white-noise ratio.*

Table 2 Received Environment Parameters

Signal	Rate	Carrier	DOA	SWNR
16-QAM	3 Mb/s	0	−45°	15 dB
BPSK	4 Mb/s	0	60°	20 dB
FDM-FM	—	−500 kHz	30°	30 dB
TV	15.625 kHz	2 Mhz	−110°	40 dB

The two PCM SOIs are spectrally self-coherent at plus-and-minus their symbol rate, with maximum self-coherence magnitude of 1/6 (−16 dB with respect to a magnitude of 1) at $\tau = 0$. In addition, the BPSK SOI is conjugate self-coherent at 0 kHz, with a maximum conjugate self-coherence strength of 1 (0 dB) at $\tau = 0$. The TV signal is also spectrally self-coherent at multiples of 15.625 kHz, out to the bandwidth of the synch pulse ($\approx$2 MHz).

The least-squares SCORE algorithm is implemented using the formula

$$r(n) = \mathbf{c}^H \mathbf{u}(n) \tag{86}$$

$$\mathbf{w}(n) = g(n)\hat{\mathbf{R}}_{xx}^{-1}(n)\hat{\mathbf{R}}_{x,r}(n), \tag{87}$$

where $g(n)$ is a power-normalizing gain variable, $\mathbf{u}(n) = \mathbf{x}^{(*)}(n)e^{j2\pi\alpha n}$ (delay = 0) and $\mathbf{c}$ is set to $[1, 0, 0, 0]^T$ (isotropic antenna pattern), and where $\hat{\mathbf{R}}_{(\cdot)}(n)$ denotes correlation with time-averaging over discrete-time collect interval $[1, n]$. The dominant mode of the cross-SCORE eigenequation is calculated using a stochastic implementation of the power method algorithm described in (41) and (42),

$$\mathbf{c}(n) = g_c(n)\hat{\mathbf{R}}_{uu}^{-1}(n)\hat{\mathbf{R}}_{ux}(n)\mathbf{w}(n-1) \tag{88}$$

$$\mathbf{w}(n) = g_w(n)\hat{\mathbf{R}}_{xx}^{-1}(n)\hat{\mathbf{R}}_{xu}(n)\mathbf{c}(n), \tag{89}$$

where $g_{(\cdot)}(n)$ are power-normalizing gain constants and n refers to the averaging time (and collect time) of the processor. In both cases the output signal is formed using the most recent processor weight vector $y(n) = \mathbf{w}^H(n)\mathbf{x}(n)$. The remaining modes of (35), (36) are calculated when required using a generalized eigenequation algorithm. The correlation statistics used in the weight update equations are calculated using a gain-normalized exponential growing rectangular window, with a recursive update formula given by

$$\hat{\mathbf{R}}_{zv}(n) = [1 - \mu(n)]\hat{\mathbf{R}}_{zv}(n-1) + \mu(n)\mathbf{z}(n)\mathbf{v}^H(n) \tag{90}$$

for arbitrary signals $\mathbf{z}(n)$ and $\mathbf{v}(n)$, where $\mu(n)$ is given by

$$\mu(n) = \begin{cases} \dfrac{1}{n} & \text{rectangular windowing} \\ \dfrac{\mu_\infty}{1-(1-\mu_\infty)^n} & \text{exponential windowing.} \end{cases} \tag{91}$$

The performance measure used to judge the quality of the processor output signal is the *output SINR*

$$\text{SINR} \triangleq |\mathbf{w}^H\mathbf{a}|^2 R_{ss}/\mathbf{w}^H\mathbf{R}_{ii}\mathbf{w}, \tag{92}$$

where $\mathbf{a}$ is the true direction vector of the SOI, R_{ss} is the true power of the SOI, and $\mathbf{R}_{ii}$ is the true autocorrelation matrix of the interference (noise and other signals) in the environment.

B. Performance in the Rank-1 Spectral Self-Coherence Environment

The performance of the SCORE processors in the rank-1 spectral self-coherence environment containing a single signal with self-coherence at the target α is investigated here. Figure 8 verifies the theoretical (infinite time-average)

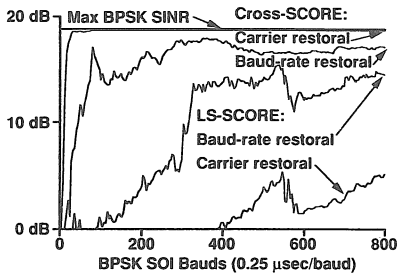

Fig. 8. SCORE performance for a BPSK SOI.

results obtained in Section III and illustrates the differing convergence rates of the least-squares SCORE and cross-SCORE processors discussed in Section III. The cross-SCORE processor converges to within 3 dB of the maximum-attainable SINR in under 100 SOI bauds in a baud-rate restoral mode ($\alpha = 4$ MHz, $\tau = 0$, conjugation disabled) and in under 20 SOI bauds in carrier restoral mode ($\alpha = 0$, $\tau = 0$, conjugation enabled). The least-squares SCORE processor converges much more slowly: the processor SINR is still 5 dB less than the maximum SINR after 350 SOI bauds in baud-rate restoral mode, and the processor fails to significantly extract the SOI after 800 SOI bauds in carrier restoral mode.

The relatively slow convergence of the least-squares SCORE processor is due to the large uncorrelated interference component $\hat{i}(t)$ present in the reference signal $r(t)$ for the choice of control vector used in this experiment. This effect is greatly reduced when the control vector is also adapted to restore self-coherence: the dominant corruption component remaining in $r(t)$ after $\mathbf{c}$ is optimized is the irreducible self-interference component (12), which is small if the self-coherence strength $|\rho_{ss(\cdot)}^{\alpha}|$ is close to unity. This also explains why the cross-SCORE processor converges much faster in carrier restoral mode than in baud-rate restoral mode: the SOI conjugate self-coherence at $\alpha = 0$ is six times stronger than the SOI spectral self-coherence at $\alpha = 4$ MHz.

The convergence of the cross-SCORE processor is not appreciably slowed by using the stochastic power-method to adapt the processor and control vectors. In fact, the difference between the processor SINR obtained using the algorithm given in (88) and (89) and the SINR obtained using the actual dominant mode of the cross-SCORE eigenequation drops to below 5 dB within 8 SOI bauds (2 μsec) in the environment used in Fig. 8 [10]. This result is consistent with the expected performance of the power-method algorithm in the rank-1 spectral self-coherence environment, because the cross-SCORE eigenequation has a very large spread between its maximum eigenvalue and its lesser eigenvalues

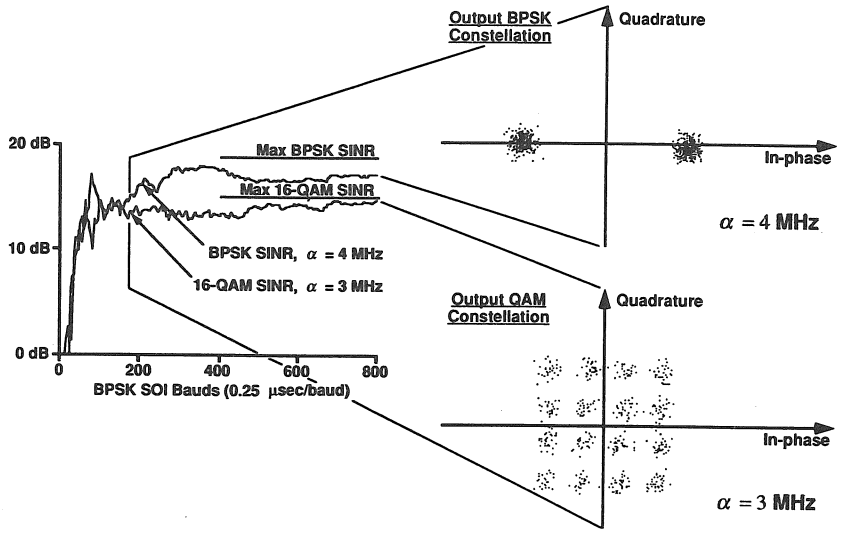

Fig. 9. Signal sorting by self-coherence frequency.

(which are all asymptotically equal to zero) in this environment.

Figure 9 demonstrates the ability of the SCORE algorithm to sort through interference environments and extract SOIs on the basis of their differing self-coherence frequencies, a key feature of the cross-SCORE processor. Removing the conjugation operation and setting the target self-coherence frequency α to 4 MHz causes the SCORE processor to select the BPSK SOI; changing α to 3 MHz causes the SCORE processor to reject the BPSK SOI and select the 16-QAM SOI. In both cases, the processor converges to within 3 dB of the optimal performance within 100 (BPSK) SOI bauds.

Figure 10 illustrates the ability of the rectangularly windowed SCORE processor to tolerate error in the assumed

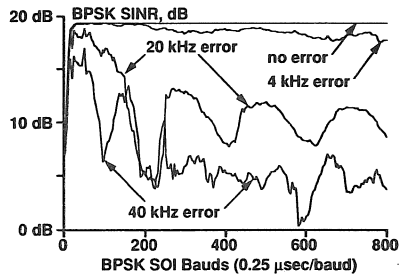

Fig. 10. Tolerance of rectangularly-windowed cross-SCORE to target self-coherence error.

SOI self-coherence frequency, a particularly important problem when conjugate self-coherence (which is affected by Doppler shift) is being restored by the processor. The processor is implemented here in carrier-restoral mode (conjugation enabled, $\tau = 0$) for varying amounts of error in the target α. In all cases where α is in error, the processor eventually rejects the BPSK SOI; as Fig. 10 shows, however, the time required for this to happen is long when the error is small. Furthermore, even when the error is large and the rejection time is short, the SINR of the selected SOI can reach a high value before the SCORE processor begins to reject the SOI. In many applications, this SINR may be high enough to allow a more robust (but less discriminatory) algorithm, such as a constant modulus algorithm, to take over adaptation of the array. Alternately, the rejection time may be long enough to allow the error in α to be estimated and removed over the SOI transmission time.

The simulation performed in Fig. 10 is repeated in [10] using the exponential windowing algorithm given in (91), for $0.001 \leq \mu_\infty \leq 0.1$, in order to evaluate the tolerance of this window to error in the self-coherence frequency of the SOI. It is found that an exponential window can improve the tolerance of the SCORE algorithm, but at significant cost in misadjustment error. For the largest exponential decay factor chosen in [10] ($\mu_\infty = 0.1$), for instance, the SCORE algorithm experienced an average SINR loss of 6 dB below the maximum-attainable SINR for this example, for virtually all of the self-coherence errors considered in Fig. 10. However, this SINR loss fluctuated widely over the collection interval, varying by as much as 8 dB from that average value over the run-time of the simulation. It is hoped that more sophisticated averaging windows can reduce this misadjustment and increase the tolerance of the SCORE algorithm to self-coherence error.

C. *Performance in the Rank-L_α Spectral Self-Coherence Environment*

The performance of the SCORE processors in the rank-L_α spectral self-coherence environment containing L_α signals with spectral self-coherence at the target α is investigated here. Two environments are of particular interest: the *multipath* environment, where L_α correlated signals (reflections) with self-coherence at α are impinging on the array, and the *multiple-SOI* environment, where L_α uncorrelated signals with equal self-coherence strength at the same α are impinging on the array. The cross-SCORE processor is shown to reject interference and background noise, leaving at worst an arbitrary linear combination of the L_α self-coherent signals in both environments. In addition, the cross-SCORE and phase-SCORE processors are shown to sort through the multiple-SOI environment and separate the self-coherent signals with near-optimal SINR, if those signals have differing self-coherence strength at the same α (if the cross-SCORE algorithm is used), or if the signals have differing complex value (strength or phase) at the same α (if the phase-SCORE algorithm is used).

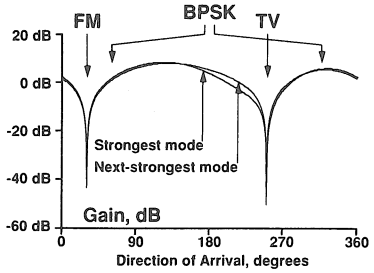

Fig. 11. Antenna pattern of most-dominant cross-SCORE solutions, multipath environment.

Figure 11 demonstrates the screening property of the cross-SCORE processor in a multipath environment where the 16-QAM signal in Table 2 has been replaced by a one-sample (50 nsec) delayed replica of the BPSK signal listed in that table. The delayed-path signal $s(t - \tau_d)$ is almost fully correlated with the direct-path signal $s(t)$, ($|\rho_{ss}(\tau_d)| = 0.93$) for this value of delay, presenting a difficult extraction problem for any processor operating without prior knowledge of the signal DOAs. However, Fig. 11 shows that the two most-dominant modes of the cross-SCORE eigenequation are able to reject the interference signals that are not self-coherent at the SOI symbol rate, and to pass some linear combination of the two SOI components. In [10] it is also shown that SOI components are extracted with significant distortion, but without the cancellation effects observed in multipath environments with other blind techniques such as power-minimization techniques.

Figure 12 demonstrates the ability of the cross-SCORE processor to sort through interference environments and extract signals on the basis of their differing self-coherence strengths. The cross-SCORE processor is configured here in baud-rate restoral mode, and the 16-QAM signal listed in Table 2 has been replaced with a 4 Mb/s BPSK signal with 50% Nyquist rolloff. This environment therefore contains two BPSK signals with spectral self-coherence at 4 MHz but with differing self-coherence strengths (1/6 for the signal with 100% rolloff, and 1/14 for the signal with 50% rolloff). Figure 12 shows that the eigenvector corresponding to the largest eigenvalue of (35) selects the BPSK signal with 100% Nyquist rolloff, while the eigenvector corresponding to the next-largest eigenvalue of (35) selects the BPSK signal with 50% Nyquist rolloff. In each case, the SINR of the selected signal converges to within 3 dB of its maximum attainable value.

Figures 13 and 14 illustrate the performance of the SCORE processors when the self-coherent signals have equal self-

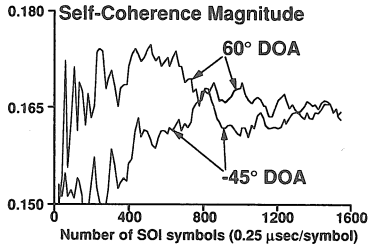

Fig. 13. Measured SOI self-coherence magnitudes for two i.i.d. BPSK received signals.

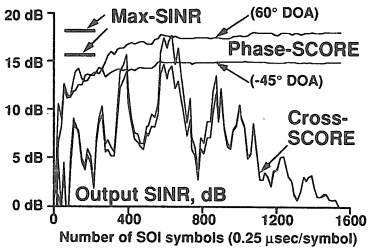

Fig. 14. Output cross-SCORE, phase-SCORE SINRs for two i.i.d. BPSK received signals.

coherence strengths. The cross-SCORE processor is implemented here with the conjugation disabled and $\alpha = 4$ MHz, and with the 16-QAM signal listed in Table 2 replaced by a BPSK signal with the same structure as the BPSK signal given in that table, but with a different timing phase and a statistically independent bit sequence. This environment then contains two independent and identically distributed (i.i.d.) signals with identical self-coherence strengths of 1/6 at $\alpha = 4$ MHz and $\tau = 0$. However, the two BPSK signals

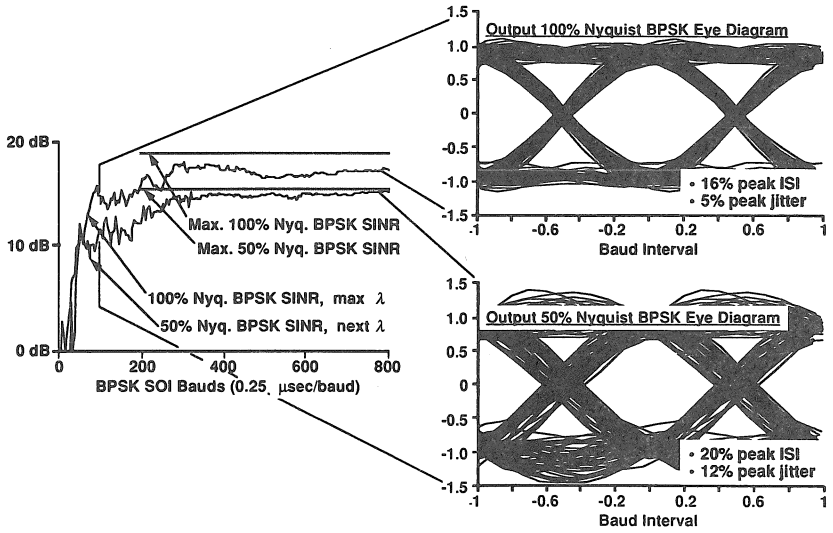

Fig. 12. Signal sorting by eigenequation solution.

have differing self-coherence phases, due to their differing timing phases.

Figure 13 shows that the *estimated* self-coherence strengths of the transmitted BPSK SOIs do not begin to settle about their expected values until roughly 800 data bauds have been collected. Comparison of Fig. 13 with the SINR of the two highest-eigenvalue solutions shown in Fig. 14 reveals that the cross-SCORE processor separates the two SOIs until their estimated self-coherence strengths become too close. After this point, the dominant modes no longer separate the SOIs, but continue to reject the interference and pass some linear combination of the two SOIs (plus a low level background of noise and residual interference). In contrast, Fig. 14 shows that an auto-SCORE algorithm such as the phase-SCORE algorithm can select and separate the BPSK signals even after the estimated self-coherence strengths of the SOIs have converged to the same value. The phase-SCORE algorithm is able to select each of the SOIs with near-optimal output SINR in this environment, by exploiting the differing self-coherence phase of these signals. The phase-SCORE SINR curves are also much smoother in Fig. 14, demonstrating none of the drop-outs exhibited by the cross-SCORE algorithm in this experiment.

VI. Conclusions

A new class of algorithms for blind adaptation of antenna arrays, the *spectral self-coherence restoral (SCORE)* algorithms, is presented. Three new adaptive processors, the *least-squares SCORE processor*, the *cross-SCORE processor*, and the *auto-SCORE processors*, are developed, analyzed, and simulated in the *rank-1* and *rank-L_α* spectral self-coherence environments where 1 and L_α signals with spectral self-coherence or conjugate self-coherence at a known value of frequency shift and arbitrary interference without self-coherence at that value of frequency-shift are received by an antenna array. It is shown analytically and by computer simulation that the SCORE processors can select a SOI with maximum SINR in the rank-1 spectral self-coherence environment, given only knowledge of a self-coherence frequency of the SOI, for example, knowledge of the SOI symbol-rate or carrier frequency. It is also that the cross-SCORE processor can select SOIs even if their self-coherence frequencies are only approximately known, and that the cross-SCORE processor can select SOIs with near-optimum SINR in the rank-L_α spectral self-coherence environment. These properties are used to demonstrate the ability of the SCORE processor to sort through environments to extract and separate multiple PCM SOIs on the basis of their differing symbol-rates, or (if their symbol rates are equal) on the basis of their differing self-coherence strengths or phases.

These results show that the SCORE approach provides a promising alternative to existing blind adaptation techniques. The SCORE processors have unambiguous and analytically tractable convergence and selection properties, giving them an advantage over other property restoral techniques in automatic processing applications. The SCORE algorithms also operate without knowledge of the background noise or interference covariance matrix, and without knowledge of (or constraints on) the sensor array geometry or individual sensor characteristics, giving them cost, complexity and performance advantages over techniques that exploit only the spatial coherence. The highly discriminatory signal-selection properties of the SCORE approach make it ideal for directed-search applications where a few SOIs with well-known modulation properties must be extracted from dense interference environments.

References

[1] J. R. Treichler and B. G. Agee, "A new approach to multipath correction of constant modulus signals," *IEEE Trans. ASSP*, vol. ASSP-31, pp. 459–472, Apr. 1983.

[2] R. P. Gooch and J. Lundel, "The CM array: An adaptive beamformer for constant modulus signals," in *Proc. 1986 Int. Conf. on ASSP*, pp. 2523–2526, 1986.

[3] L. J. Griffiths and M. J. Rude, "The P-vector algorithm: A linearly constrained point of view," in *Proc. 20th Asilomar Conf. on Signals, Systems and Computers*, pp. 457–461, 1986.

[4] R. O. Schmidt, "Multiple emitter location and signal parameter estimation," *IEEE Trans. Antennas Propagat.*, vol. AP-34, pp. 276–280, Mar. 1986.

[5] A. Paulraj, R. Roy, and T. Kailath, "Estimation of signal parameters via rotational invariance techniques—ESPRIT," in *Proc. 19th Asilomar Conf. on Circuits, Systems and Computers*, pp. 83–89, 1985.

[6] W. A. Gardner, *Statistical Spectral Analysis: A Nonprobabilistic Theory*. Englewood Cliffs, NJ: Prentice-Hall, 1987.

[7] W. A. Gardner, *Introduction to Random Processes with Applications to Signals and Systems*, 2nd ed. New York: McGraw-Hill, 1990.

[8] B. G. Agee, S. V. Schell, and W. A. Gardner, "Self-Coherence Restoral: A New Approach to Blind Adaptation of Antenna Arrays," in *Proc. 21st Asilomar Conf. on Signals, Systems and Computers*, pp. 589–593, 1987.

[9] G. W. Stewart, *Introduction to Matrix Computations*. New York, NY: Academic Press, 1973.

[10] B. G. Agee, "The property restoral approach to blind adaptive signal extraction," Ph.D. dissertation, Dept. of Electrical Engineering and Computer Science, Univ. of California, Davis, CA, 1989.

[11] S. V. Schell and B. G. Agee, "Application of the SCORE algorithm and SCORE extensions to sorting in the rank-L environment," in *Proc. 22nd Asilomar Conference on Signals, Systems and Computers*, pp. 274–278, 1988.

Brian G. Agee (Member, IEEE) received the B.S. degree in mathematics in 1977, and the B.S., M.S., and Ph.D. degrees in electrical engineering in 1977, 1985, and 1989, respectively, all from the University of California, Davis.

From 1979 to 1984, he was a Member of Technical Staff at ARGOSystems, Inc., in Sunnyvale, CA, where he worked on problems in blind adaptive processing, direction finding, system and environment analysis, cyclic spectrum analysis, and spread spectrum communications. From 1984 to 1986 and in 1989, he was a Research Assistant, Associate-in-Engineering, and Post Graduate Research Engineer at the University of California, Davis, where he worked on problems in adaptive signal extraction and analysis. Since 1984, he has also been an independent consulting engineer, working in the areas of direction finding, cyclic spectrum analysis, and blind adaptive signal processing. His current research interests are in the area of blind adaptive signal extraction and signal analysis, with emphasis on techniques for exploiting modulation properties of the transmitted signal waveforms.

Dr. Agee is a member of NSPE, AOC, Tau Beta Pi, and Pi Mu Epsilon. He is a registered Professional Engineer in the State of California.

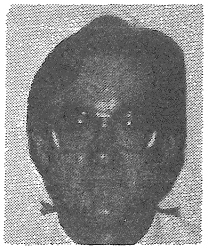

Stephan V. Schell (Student Member, IEEE) was born in Livermore, California, on March 29, 1964. He received the B.S. degree with highest honors in 1986 and the M.S. degree in 1987, both in electrical engineering, from the University of California, Davis.

From 1981 to 1986, he developed software for the solution of differential equations at Science Application International Corp. and Lawrence Livermore National Laboratory. In the summer of 1986, he worked on implementation issues in digital signal processing as a Design Engineer with Electronic Support Systems. During his graduate study, he was a UCD MICRO Fellow (1986–87) and a UCD Graduate Fellow (1987–88). As a UCD Regents Fellow, he is currently pursuing the Ph.D. degree in electrical engineering at the University of California, Davis, where he is also a Research Assistant. His research interests are in the areas of statistical signal processing, communications, and scientific computing, with emphasis on signal and parameter estimation.

Mr. Schell received the UCD Distinguished Scholar Research Award in 1987. He is a member of Tau Beta Pi, Pi Mu Epsilon, and Phi Kappa Phi.

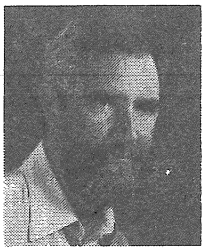

William A. Gardner (Senior Member, IEEE) was born in Palo Alto, California on November 4, 1942. He received the M.S. degree from Stanford University in 1967, and the Ph.D. degree from the University of Massachusetts, Amherst, in 1972, both in electrical engineering.

He was a Member of the Technical Staff at Bell Laboratories in Massachusetts from 1967 to 1969. He has been a faculty member at the University of California, Davis, since 1972, where he is Professor of Electrical Engineering and Computer Science. Since 1982, he has been President of the engineering consulting firm Statistical Signal Processing, Inc., Yountville, California. His research interests are in the general area of statistical signal processing, with primary emphasis on the theories of time-series analysis, stochastic processes, and signal detection and estimation.

Professor Gardner is the author of *Introduction to Random Processes with Applications to Signals and Systems*, (Macmillan, 1985, 2nd ed., McGraw-Hill, 1990), *The Random Processes Tutor* (McGraw-Hill, 1990), and *Statistical Spectral Analysis: A Nonprobabilistic Theory* (Prentice-Hall, 1987). He holds several patents and is the author of more than 50 research-journal papers. He received the Best Paper Award from the European Association for Signal Processing in 1986, the 1987 Distinguished Engineering Alumnus Award from the University of Massachusetts, and the Stephen O. Rice Prize Paper Award in the Field of Communication Theory from the Communications Society of the IEEE in 1988. He is a member of the American Mathematical Society, the Mathematical Association of America, the American Association for the Advancement of Science, the European Association for Signal Processing, Tau Beta Pi, Eta Kappa Nu, and Alpha Gamma Sigma.